NONWOVENS: MELT- AND SOLUTION BLOWING

A.L. Yarin

Mechanical & Industrial Engineering

Department of Mechanical Eng. UIC, Chicago

Acknowledgement

- **The Nonwovens Cooperative Research Center (NCRC), USA**

Collaboration with:

PhD student S. Sinha-Ray

NC State: Prof. B. Pourdeyhimi

Mechanical & Industrial Engineering

Outline

1. Meltblowing
2. Experimental: Solid flexible threadline in parallel high speed gas flow
3. Turbulence, bending perturbations, their propagation and flapping
4. Theoretical: Solid flexible threadline in parallel high speed gas flow
5. Comparison between theory and experiment
6. Theoretical: Polymer viscoelastic liquid jets in parallel high speed gas flow
7. Fiber-size distribution
8. Fiber orientation distribution in laydown
9. Spatial mass distribution in laydown
10. Experiments with solution blowing and co-blowing of core-shell and hollow fibers

My book published in 1993 by Longman (U.K.) and Wiley&Sons (New York) encompasses all relevant equations and a number of relevant solutions for free liquid jets moving in air

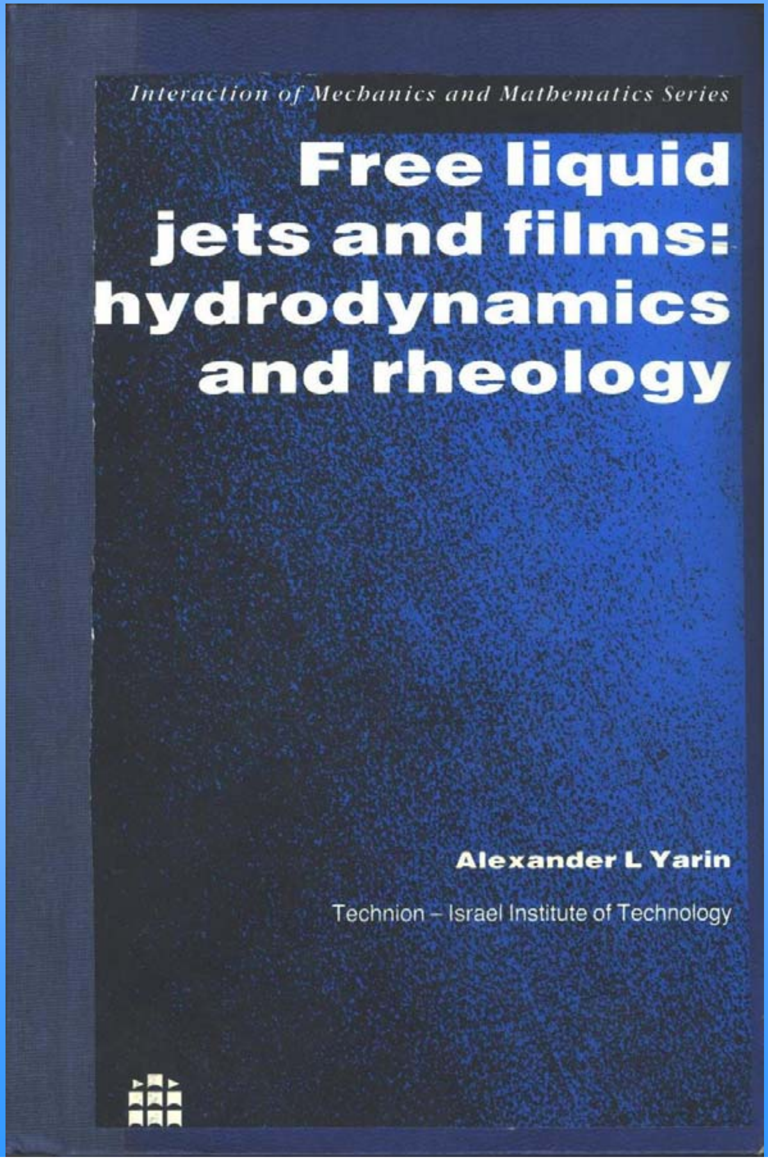

Mechanical & Industrial Engineering

General quasi-one-dimensional equations of dynamics of free liquid jets moving in air

1. Continuity-Mass Balance- Equation

$$\frac{\partial \lambda f}{\partial t} + \frac{\partial f W}{\partial s} = 0$$

All terms in Eq. (1) are of the order of **a^2**

2. Momentum Balance Equation

$$\frac{\partial \lambda f \mathbf{V}}{\partial t} + \frac{\partial f W \mathbf{V}}{\partial s} = \frac{1}{\rho} \frac{\partial \left(P\tau + \mathbf{Q} \right)}{\partial s} + \lambda f \mathbf{g} + \frac{\lambda}{\rho} \mathbf{q}_{\text{total}}$$

All terms in Eq. (2) except the shearing force **Q** are of the order of **a^2 ;**
Q is of the order of **a^4**

Mechanical & Industrial Engineering

General quasi-one-dimensional equations of dynamics of free liquid jets moving in air

3. The Moment-of-Momentum Balance- Equation

$$\frac{\partial \lambda \mathbf{K}}{\partial t}+\lambda\left[\mathbf{U}\times\mathbf{j}_1+\boldsymbol{\tau}\times\left(\mathrm{U}\mathbf{j}_{1\tau}+\mathbf{j}_2+\mathrm{W}\mathbf{j}_1\right)-\mathrm{k}\mathbf{U}\times\left(\boldsymbol{\Omega}\times\mathbf{j}_3+\delta\mathbf{j}_3\right)\right]$$

$$+\frac{\partial\left(\mathrm{W}\mathbf{K}_1+\mathbf{j}_4\times\mathbf{V}\right)}{\partial s}=\frac{1}{\rho}\frac{\partial\mathbf{M}}{\partial s}+\frac{1}{\rho}\lambda\boldsymbol{\tau}\times\mathbf{Q}-\lambda\mathrm{k}\mathbf{j}_3\times\mathbf{g}+\frac{\lambda}{\rho}\mathbf{m}$$

All terms in Eq. (3) are of the order of $\mathbf{a}^4$

Equations (1)-(3) are supplemented with the geometric, kinematic, and material relations. The material relations for P and M follow from the rheological constitutive equation projected on the quasi-1D kinematics

Mechanical & Industrial Engineering

Main results for highly viscous and viscoelastic jets rapidly moving in air: flame throwers

The linear stability analysis: small 3D perturbations grow with the rate:

$$\gamma^2 + \frac{3}{4}\frac{\mu\chi^4}{\rho a_0^2}\gamma + \left(\frac{\sigma}{\rho a_0^3} - \frac{\rho_a U_0^2}{\rho a_0^2}\right)\chi^2 = 0$$

where the dimensionless wavenumber $\chi = 2\pi a_0 / \ell$

The bending instability sets in when:

$$U_0 > U_0^* = \sqrt{\sigma / (\rho_a a_0)}$$

Main results for highly viscous and viscoelastic jets rapidly moving in air: flame throwers

The bending perturbations grow much faster than the capillary perturbations for highly viscous liquids when:

$$\frac{\mu^2}{\rho a_0^2 \rho_a U_0^2} >> 1$$

Linear spectrum:

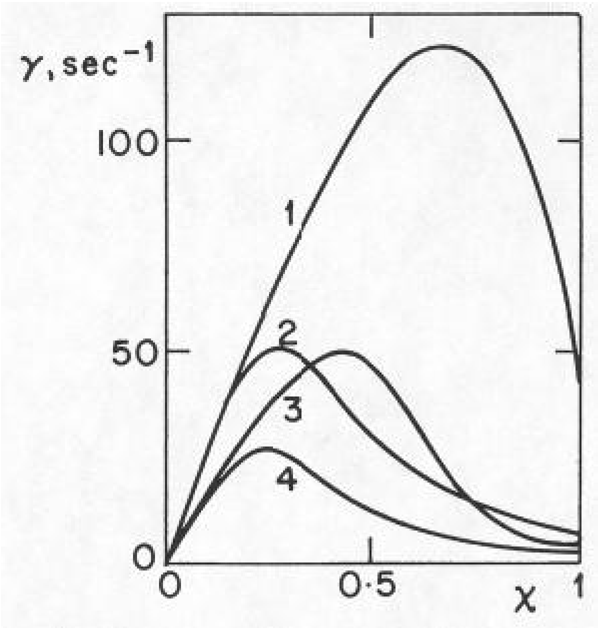

Mechanical & Industrial Engineering

Nonlinear-numerical-results for 2D bending

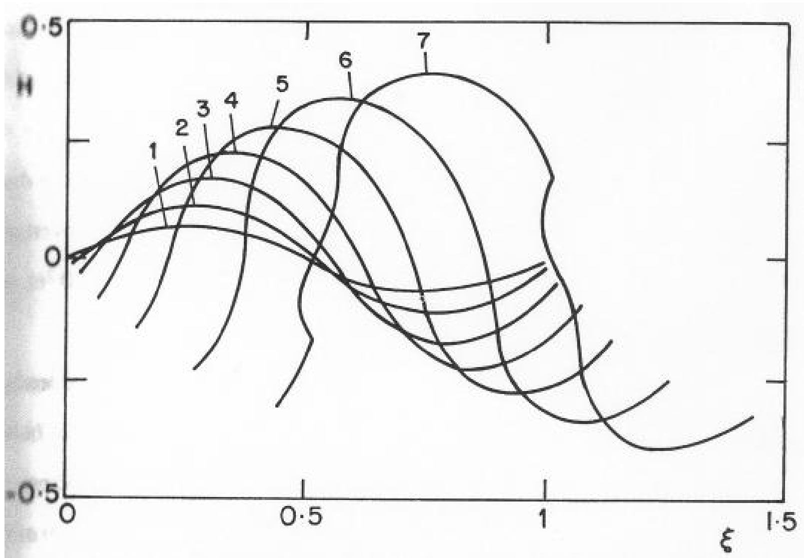

Newtonian jet

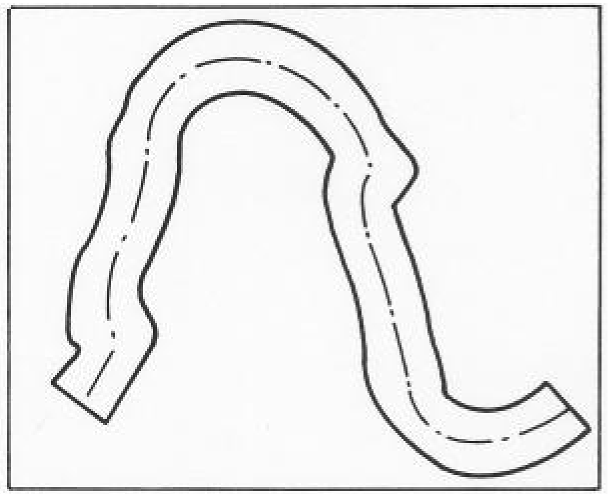

Nonlinear-numerical-results for 2D bending

Newtonian jet

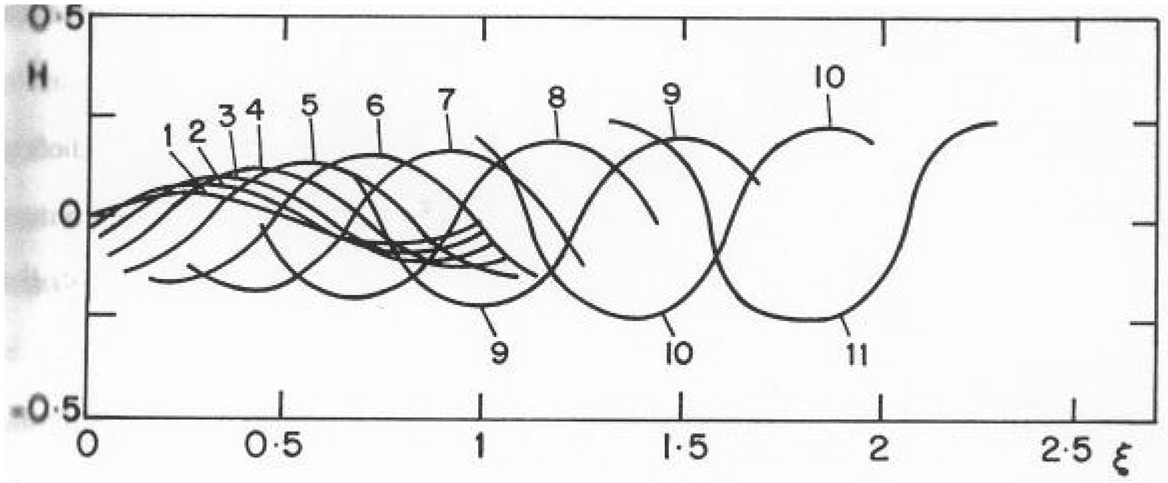

Viscoelastic jet

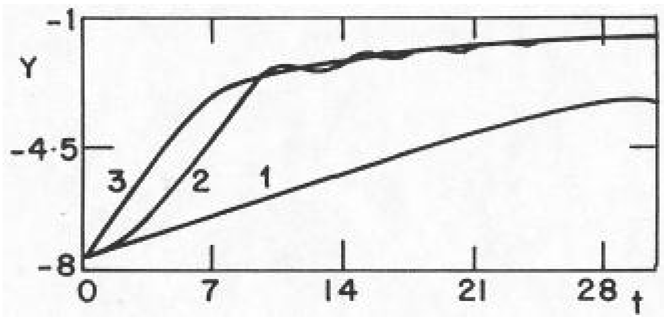

Meltblowing

Experimental: threadline blowing setup to probe turbulence

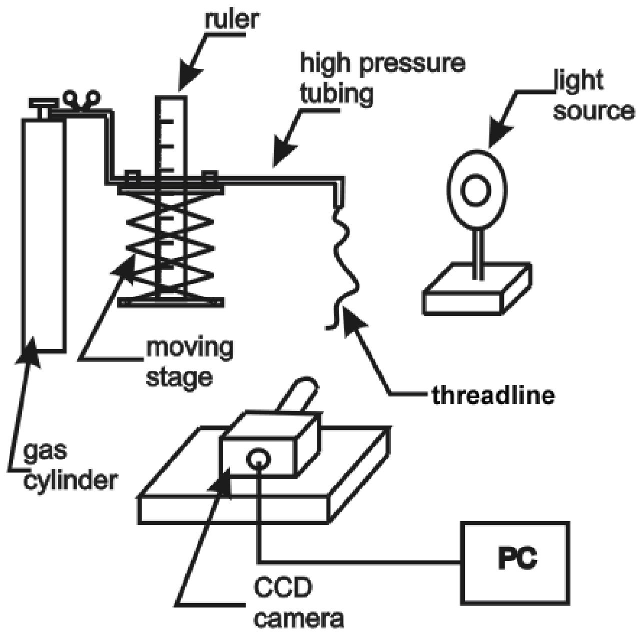

S. Sinha-Ray, A.L. Yarin, B. Pourdeyhimi.

J. Appl. Phys. 108, 034912 (2010)

Air velocity at the nozzle exit

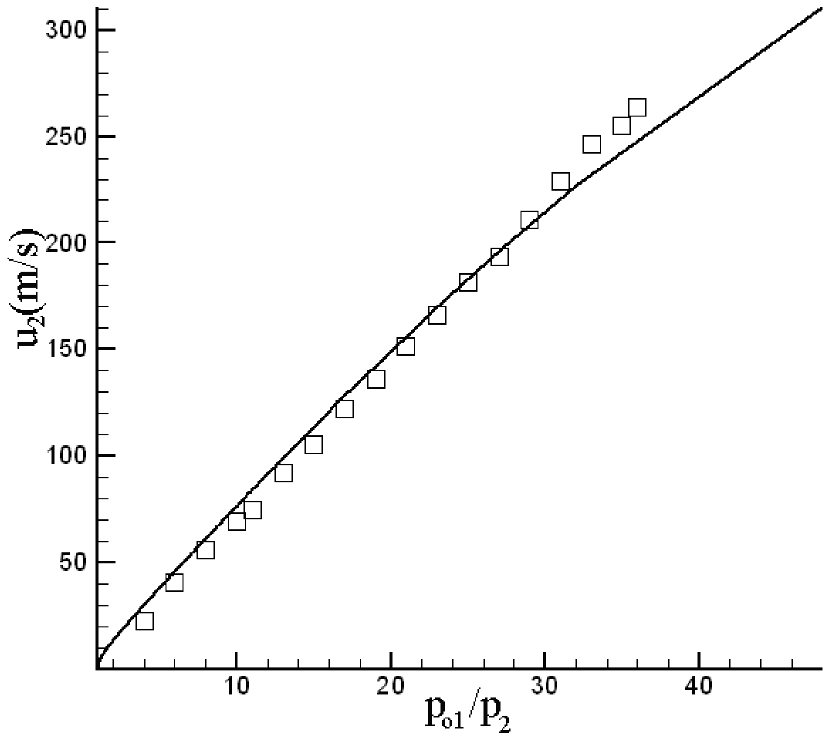

Chocking at pressure ratio of 47.91

Experimental: threadline configurations at different time moments

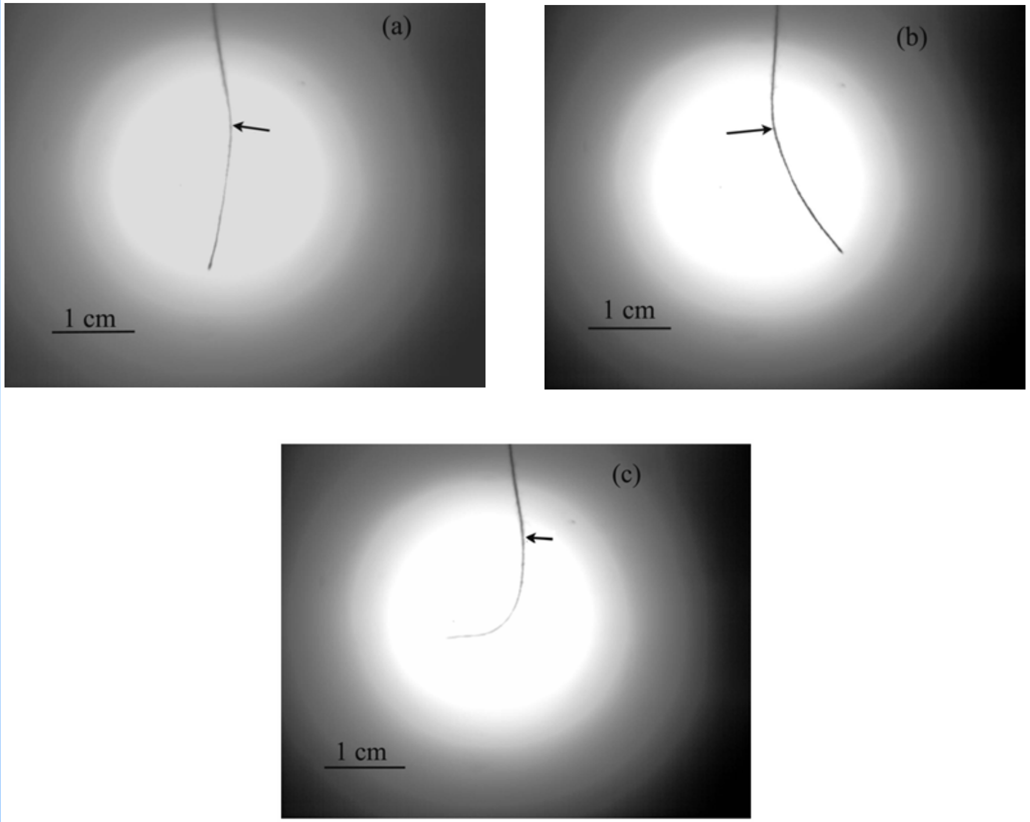

ARROWS DENOTE THE FLAPPING LENGTH

Mechanical & Industrial Engineering

Threadline envelope: 2nd method to define flapping length

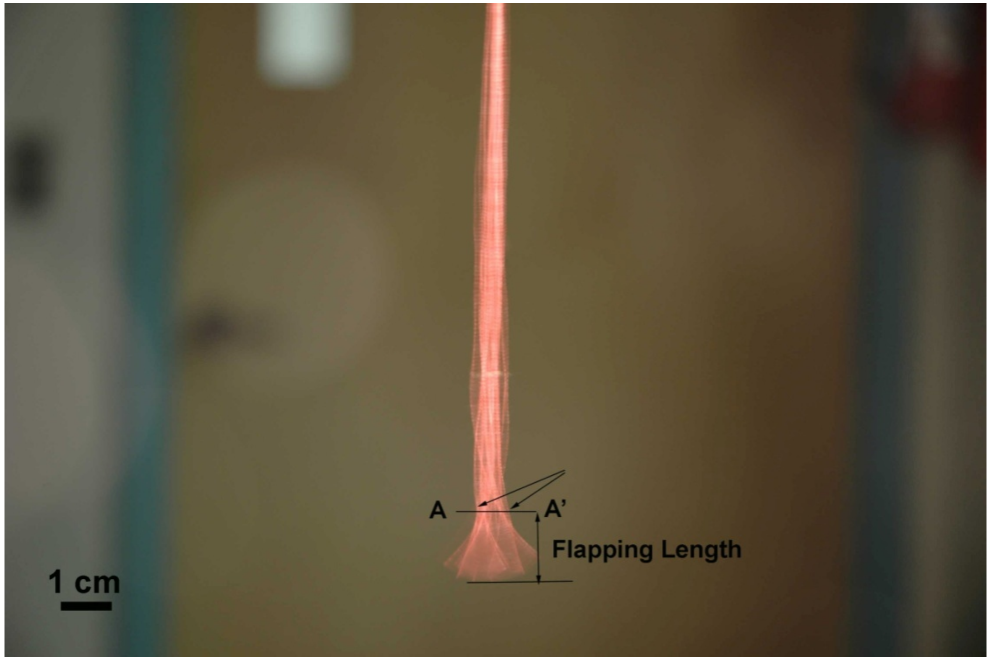

Mechanical & Industrial Engineering

Measured threadline oscillations

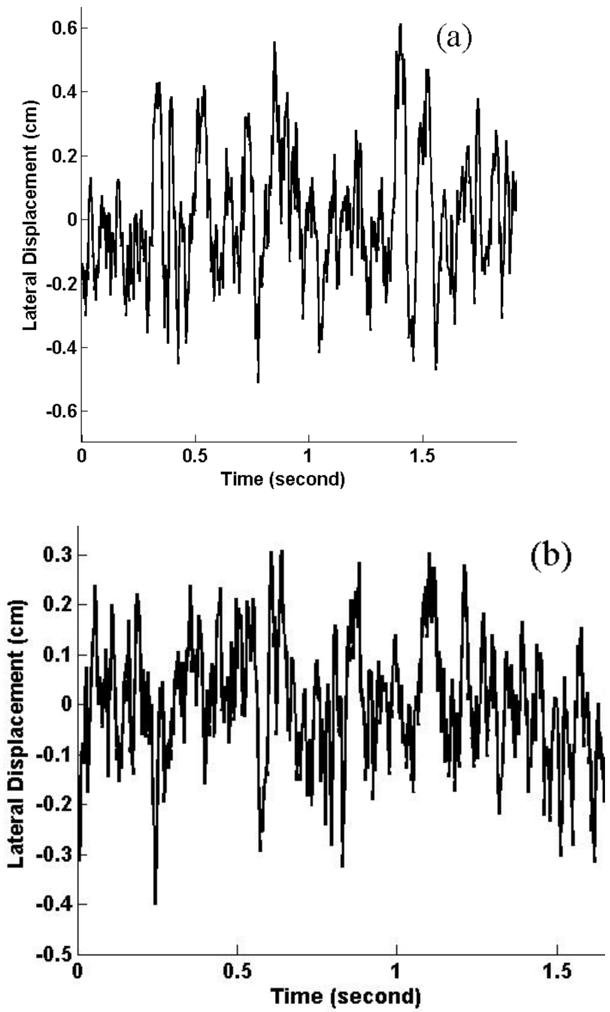

Mechanical & Industrial Engineering

FFT: Spectrum of the threadline oscillations

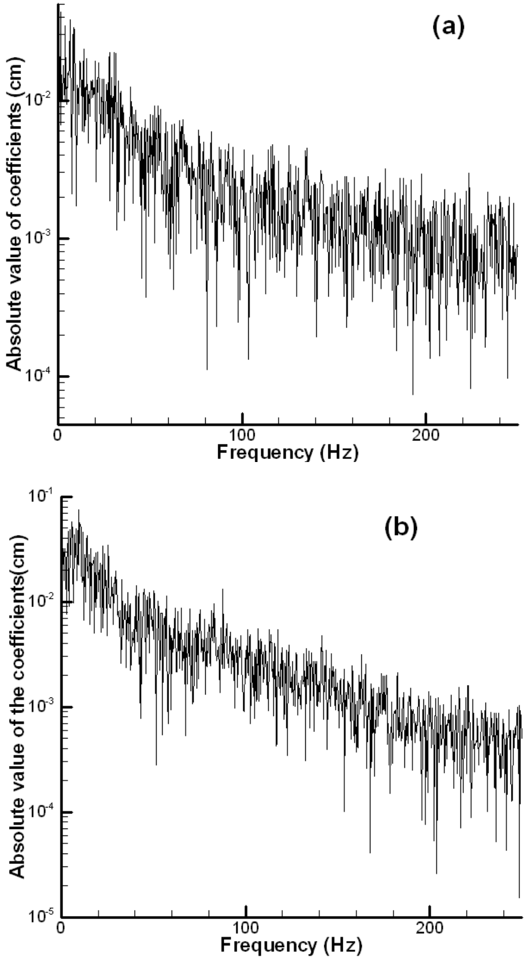

Mechanical & Industrial Engineering

Fourier reconstruction of the threadline oscillations with high frequency truncation above 167 Hz

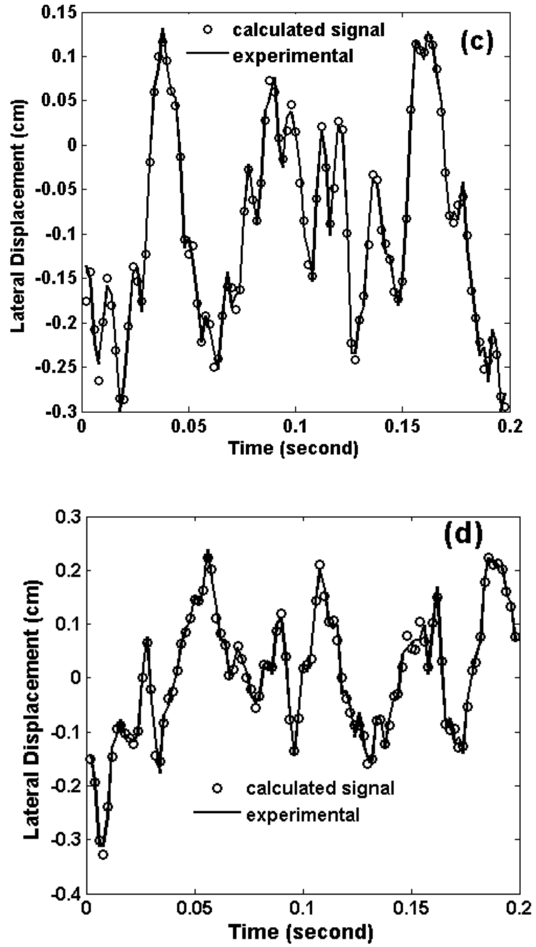

Mechanical & Industrial Engineering

Autocorrelation function: chaotic nature of threadline oscillations

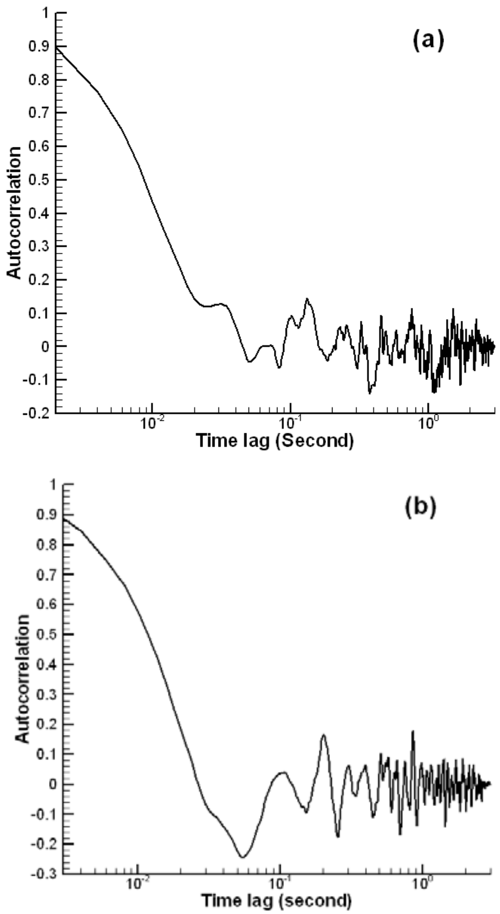

Turbulence, bending perturbations, their propagation and flapping

$$\text{Large eddy frequency}: U_0 / L = 10^3\ \text{Hz}$$

$$\text{Taylor microscale}: \lambda = 1.23\,\text{Re}_d^{-1/2}\,x \Rightarrow$$

$$\lambda = 0.014 - 0.14\ \text{cm}$$

$$\text{Microscale frequency}: U_0 / \lambda = 10^5 - 10^6\ \text{Hz}$$

$$\text{Threadline oscillation frequency}: 10 - 10^2\ \text{Hz}$$

Multiple impacts of large eddies:

$$< A >= [2 < v'^2 > \tau t]^{1/2}$$

$$v' \approx u' \Rightarrow < v'^2 >=< u'v' >$$

$$\tau \approx (\partial u / \partial y)^{-1} \Rightarrow$$

$$< v'^2 > \tau = \nu_t \ \text{turbulent eddy viscosity!}$$

Mechanical & Industrial Engineering

Turbulence, bending perturbations, their propagation and flapping

Therefore,

$$< A >= (2\nu_t t)^{1/2}$$

In axisymmetric turbulent gas jets:

$$\nu_t = 0.015 U_0 d_0 = \text{const}$$

Time t is restricted by bending perturbation propagation over the threadline:

$$t \approx L / \sqrt{P / (S\rho_{\text{threadline}})}$$

Threadline tension: $P = q_\tau L$,

which is imposed by air drag:

$$q_\tau = 0.65\pi a_0 \rho_g U_0^2 \left(\frac{2U_0 a_0}{\nu_g} \right)^{-0.81}$$

Mechanical & Industrial Engineering

Turbulence, bending perturbations, their propagation and flapping

For $U_0 = 230\ \mathrm{m/s}$, $d_0 = 0.05\ \mathrm{cm}$ in air:

$\nu_t = 17.25\ \mathrm{cm^2/s}$, $t = 0.0256\ \mathrm{s}$

Therefore, $t^{-1} = 39\,\mathrm{Hz}$ – a remarkable agreement with the data!

$< A >= (2\nu_t t)^{1/2} = 0.94\ \mathrm{cm}$ – a reasonable agreement with the data!

Mechanical & Industrial Engineering

Turbulence, bending perturbations, their propagation and flapping

The shape of the threadline envelope in the case of distributed impacts of turbulent pulsations without distributed lift force is predicted as:

$$< A(x) >= 0.16\left(\frac{\rho}{\rho_g}\right)^{1/4}\left(\frac{U_0 d_0}{\nu_g}\right)^{0.2025}\left(\frac{d_0}{L}\right)^{1/4}\frac{\sqrt{d_0 L}}{(1-x)^{1/4}}$$

i.e.

$$< A(x) >\approx \frac{1}{(1-x)^{1/4}}$$

Turbulence vs. distributed aerodynamic lift force

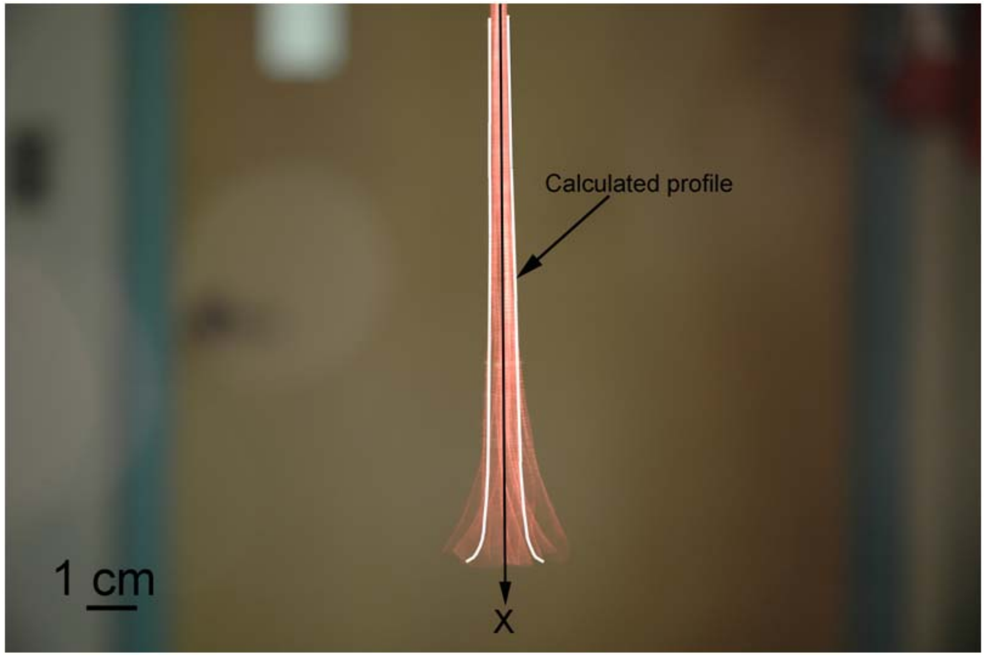

Distributed drag, lift and random forces

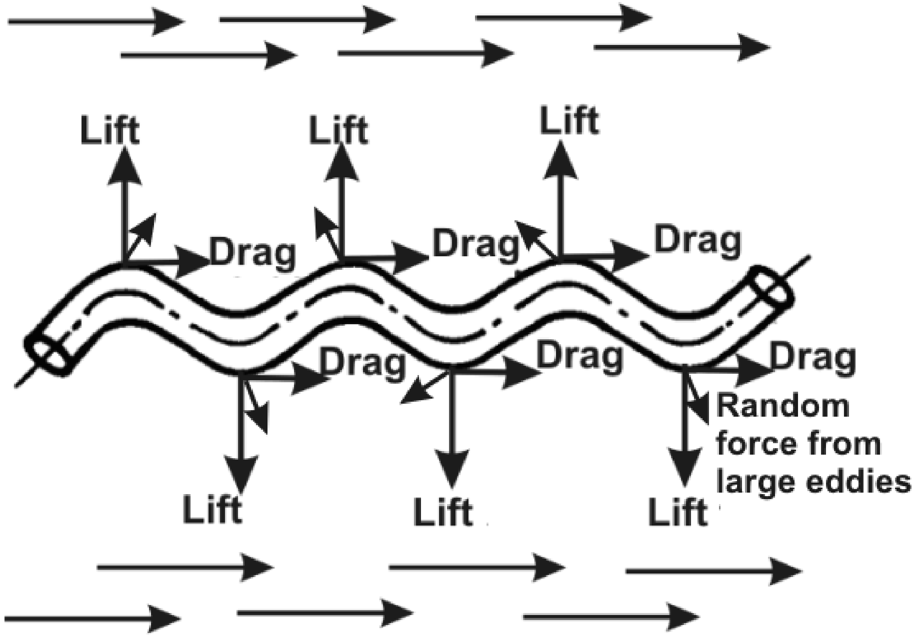

Straight unperturbed sewing threadline in high speed air flow

The unperturbed momentum balance

$$\frac{dP}{dx} + q_\tau = 0, \quad P = \sigma_{xx} \pi a_0^2$$

The longitudinal aerodynamic drag force

$$q_\tau = 0.65 \pi a_0 \rho_g U_0^2 \left(\frac{2U_0 a_0}{\nu_g} \right)^{-0.81}$$

Integrating the momentum balance, we obtain

$$\sigma_{xx} = \frac{q_\tau (L - x)}{\pi a_0^2}$$

Mechanical & Industrial Engineering

Perturbed threadline in high speed air flow

The lateral bending force

$$q_n = -\rho_g U_0^2 \pi a_0^2 \frac{\partial^2 H}{\partial x^2}$$

The linearized lateral momentum balance

$$\rho \pi a_0^2 \frac{\partial V_n}{\partial t} = kP + q_n$$

The lateral velocity and thread curvature read

$$V_n = \frac{\partial H}{\partial t}, \quad k = \frac{\partial^2 H}{\partial x^2}$$

Mechanical & Industrial Engineering

Perturbed threadline in high speed air flow

Then, the thread configuration is governed by

$$\frac{\partial^2 H}{\partial t^2} + \frac{\left[\rho_g U_0^2 - \sigma_{xx}(x)\right]}{\rho} \frac{\partial^2 H}{\partial x^2} = 0 \qquad (1)$$

If $\sigma_{xx0} = q_\tau L/(\pi a_0^2) > \rho_g U_0^2$, then Eq.(1) is hyperbolic at $0 \le x \le x_*$, and elliptic at $x_* \le x \le L$.

The transition cross-section is found from

$$\rho_g U_0^2 - \frac{q_\tau (L - x)}{\pi a_0^2} = 0 \quad @\, x = x_*$$

The threadline is clamped and perturbed at $x = 0$

$$H\big|_{x=0} = H_{0\omega} \exp(i\omega t), \;\; \partial H/\partial x\big|_{x=0} = 0$$

Mechanical & Industrial Engineering

Perturbed threadline in high speed air flow

Solution in the hyperbolic part is

$$H(x,t) = H_{0\omega} \exp(i\omega t) \cos[\omega I(x)]$$

where

$$I(x) = \frac{2\rho\pi a_0^2}{q_\tau} \left\{ \begin{aligned} & \left[\left(\frac{q_\tau L}{\pi a_0^2} - \rho_g U_0^2 \right) / \rho \right]^{1/2} \\ & - \left[\left(\frac{q_\tau (L - x)}{\pi a_0^2} - \rho_g U_0^2 \right) / \rho \right]^{1/2} \end{aligned} \right\}$$

Solution in the elliptic part is

$$H(x,t) = H_{0\omega} \exp(i\omega t) \left\{ \begin{aligned} & \cosh\left[\omega J(x)\right] \cos\left[\omega I(x_*)\right] \\ & + i \sinh\left[\omega J(x)\right] \sin\left[\omega I(x_*)\right] \end{aligned} \right\}$$

where

$$J(x) = \frac{2\rho\pi a_0^2}{q_\tau} \left[\frac{q_\tau x}{\rho\pi a_0^2} - \frac{q_\tau L/(\pi a_0^2) - \rho_g U_0^2}{\rho} \right]^{1/2}$$

Mechanical & Industrial Engineering

Flapping of solid flexible threadline

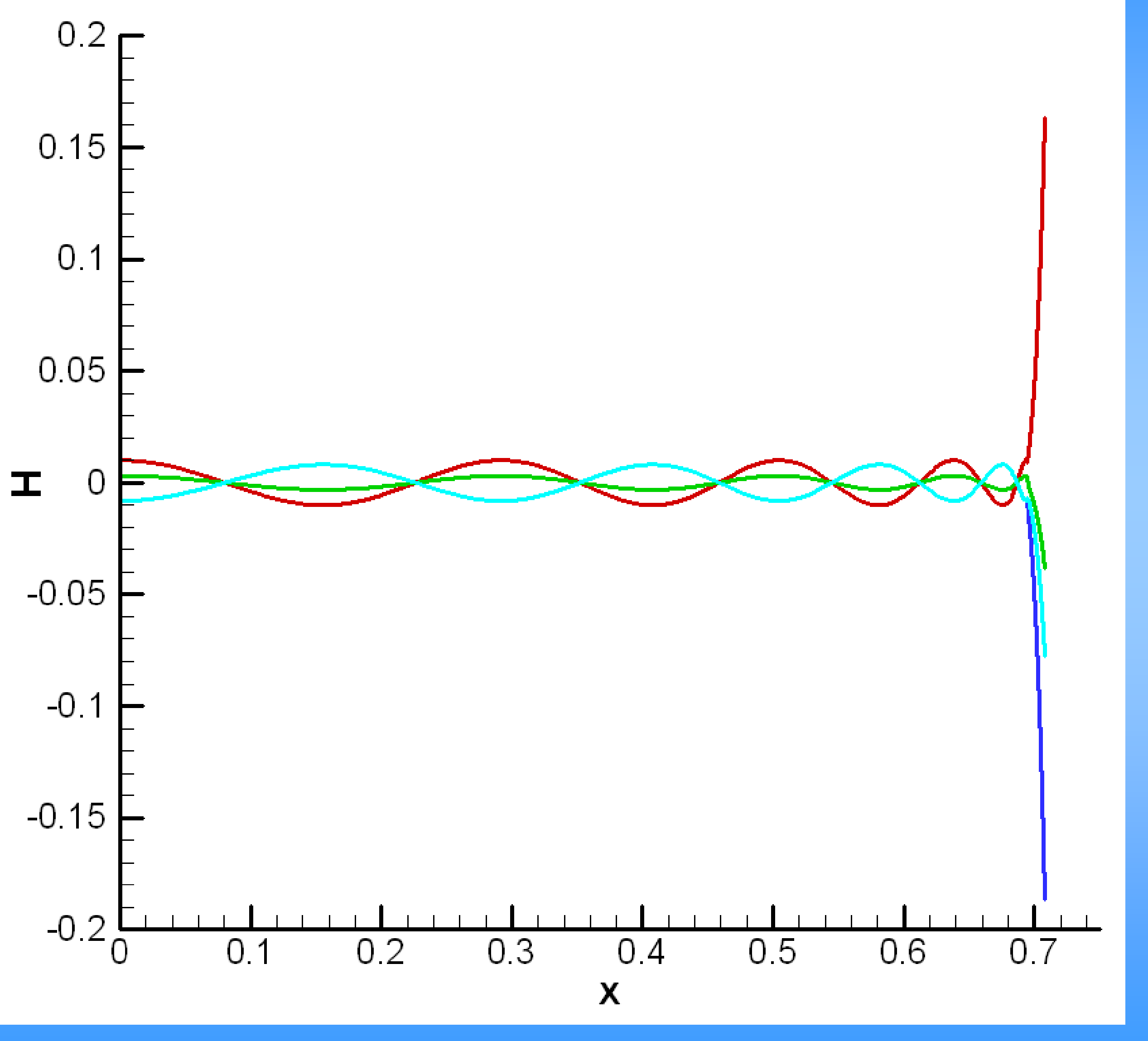

Theory vs. experiments for threadline

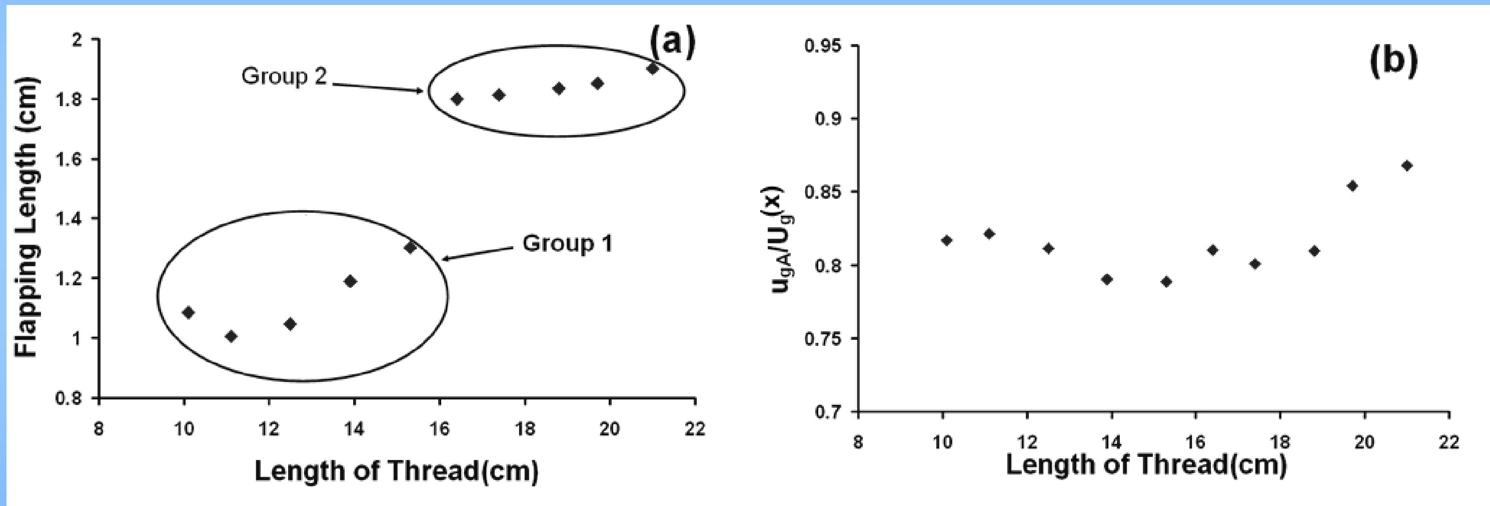

Theory vs. experiments for threadline

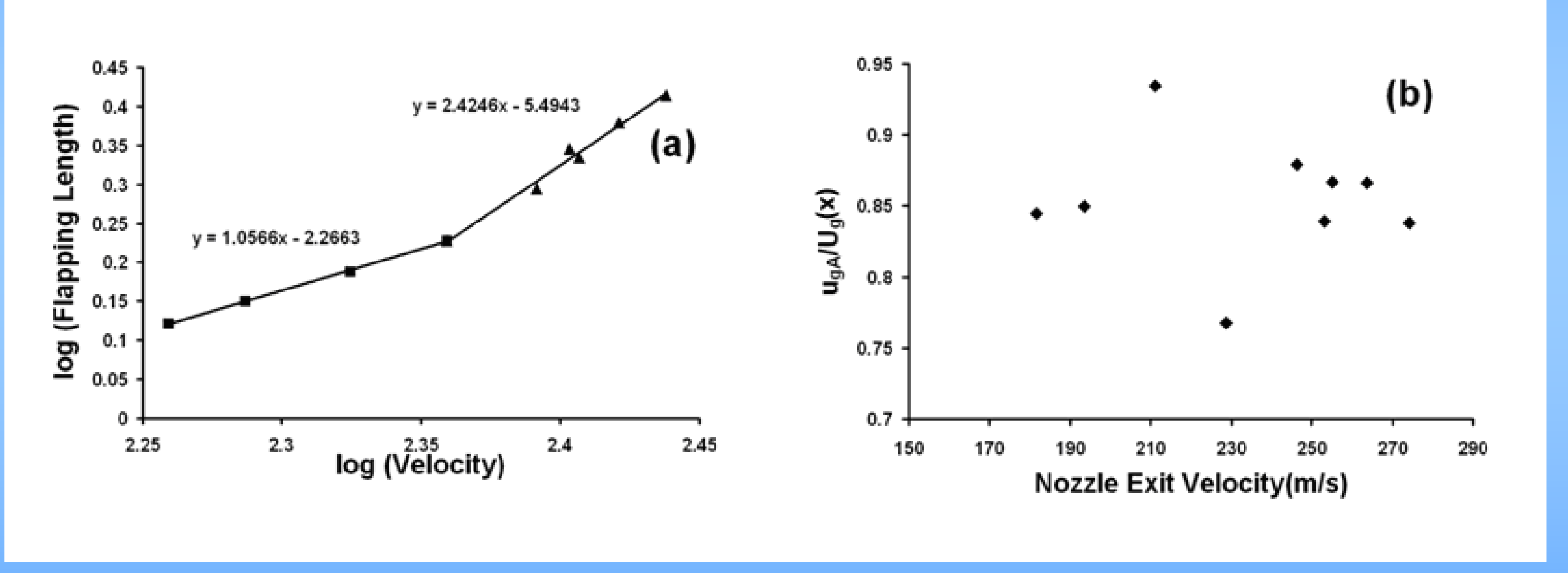

Mechanical & Industrial Engineering

Polymeric liquid jet in high speed air flow

The quasi – one – dimensional continuity and momentum balance equations for a straight jet

$$\frac{dfV_\tau}{dx} = 0, \quad f = \pi a^2 \Rightarrow \pi a^2 V_\tau = \pi a_0^2 V_{\tau 0}$$

$$\rho \frac{dfV_\tau^2}{dx} = \frac{d\sigma_{xx} f}{dx} + q_\tau$$

where

$$q_\tau = 0.65\pi a \rho_g (U_g - V_\tau)^2 \left[\frac{2(U_g - V_\tau)a}{\nu_g} \right]^{-0.81}$$

and the stress $\sigma_{xx} = \tau_{xx} - \tau_{yy}$ is found from

Polymeric liquid jet in high speed air flow

The upper – convected Maxwell model of viscoelasticity

$$V_\tau \frac{d\tau_{xx}}{dx} = 2\frac{dV_\tau}{dx}\tau_{xx} + \frac{2\mu}{\theta}\frac{dV_\tau}{dx} - \frac{\tau_{xx}}{\theta}$$

$$V_\tau \frac{d\tau_{yy}}{dx} = -\frac{dV_\tau}{dx}\tau_{yy} - \frac{\mu}{\theta}\frac{dV_\tau}{dx} - \frac{\tau_{yy}}{\theta}$$

which are solved numerically simultaneously with the transformed momentum balance.

The following dimensonless groups are used

$$R = \frac{\rho_g}{\rho}, \quad \ell = \frac{L}{a_0}, \quad \mathrm{Re} = \frac{2V_\tau^0 a_0}{\nu_g}, \quad \mathrm{De} = \frac{\theta V_{\tau 0}}{L}$$

$$E = \frac{2R}{\mathrm{De}\,\ell\,\mathrm{Re}\,M}, \quad M = \frac{\mu_g}{\mu}$$

Mechanical & Industrial Engineering

Polymeric liquid jet in high speed air flow

The dimensionless equations for a straight polymeric jet solved numerically

$$\frac{dV_\tau}{dx} = \frac{\left[-E(\tau_{xx} - \tau_{yy})/(DeV_\tau^2) + q_\tau\right]}{\left[1 - E(\tau_{xx} + 2\tau_{yy} + 3)/V_\tau^2\right]}$$

$$\frac{d\tau_{xx}}{dx} = \frac{1}{V_\tau}\left(2\frac{dV_\tau}{dx}\tau_{xx} + 2\frac{dV_\tau}{dx} - \frac{\tau_{xx}}{De}\right)$$

$$\frac{d\tau_{yy}}{dx} = \frac{1}{V_\tau}\left(-\frac{dV_\tau}{dx}\tau_{yy} - \frac{dV_\tau}{dx} - \frac{\tau_{yy}}{De}\right)$$

The boundary conditions are

$$x = 0: \quad V_\tau = 1, \quad \tau_{xx} = \tau_{xx0}, \quad \tau_{yy} = 0$$

Mechanical & Industrial Engineering

Unperturbed polymer jet in melt blowing: velocity and radius distributions

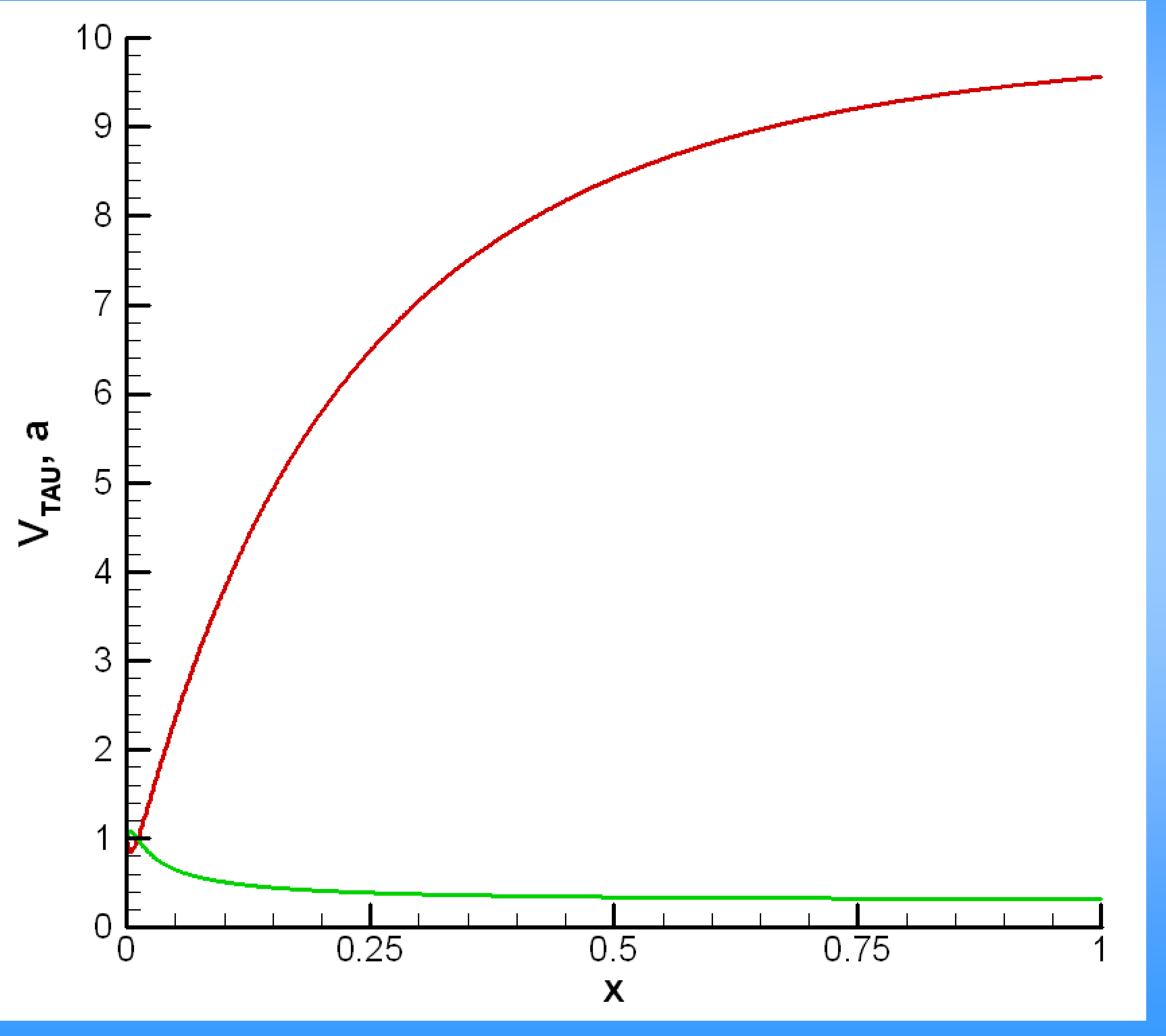

Mechanical & Industrial Engineering

Unperturbed polymer jet in melt blowing: longitudinal deviatoric stress distribution

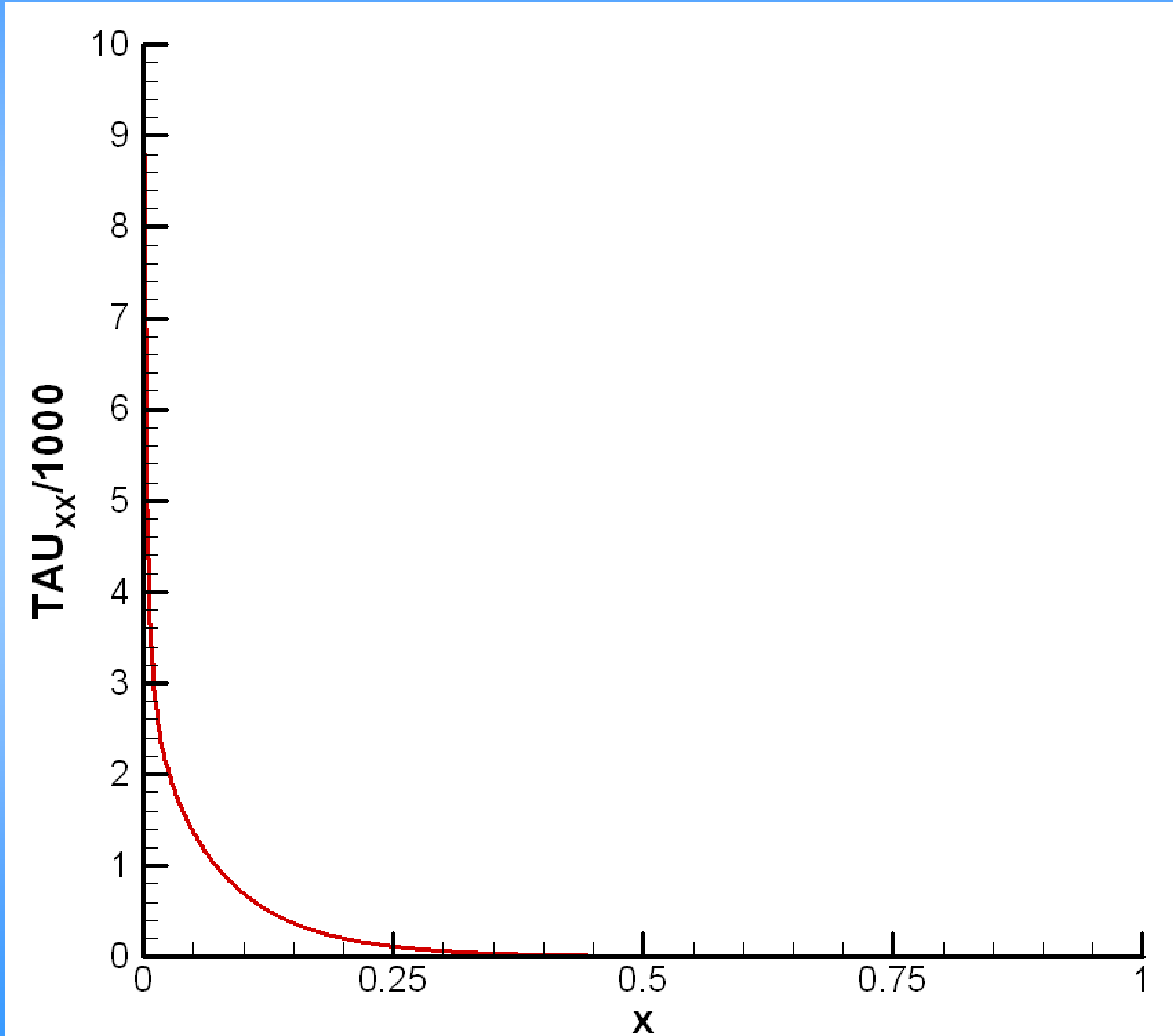

Unperturbed polymer jet in melt blowing: lateral deviatoric stress distribution

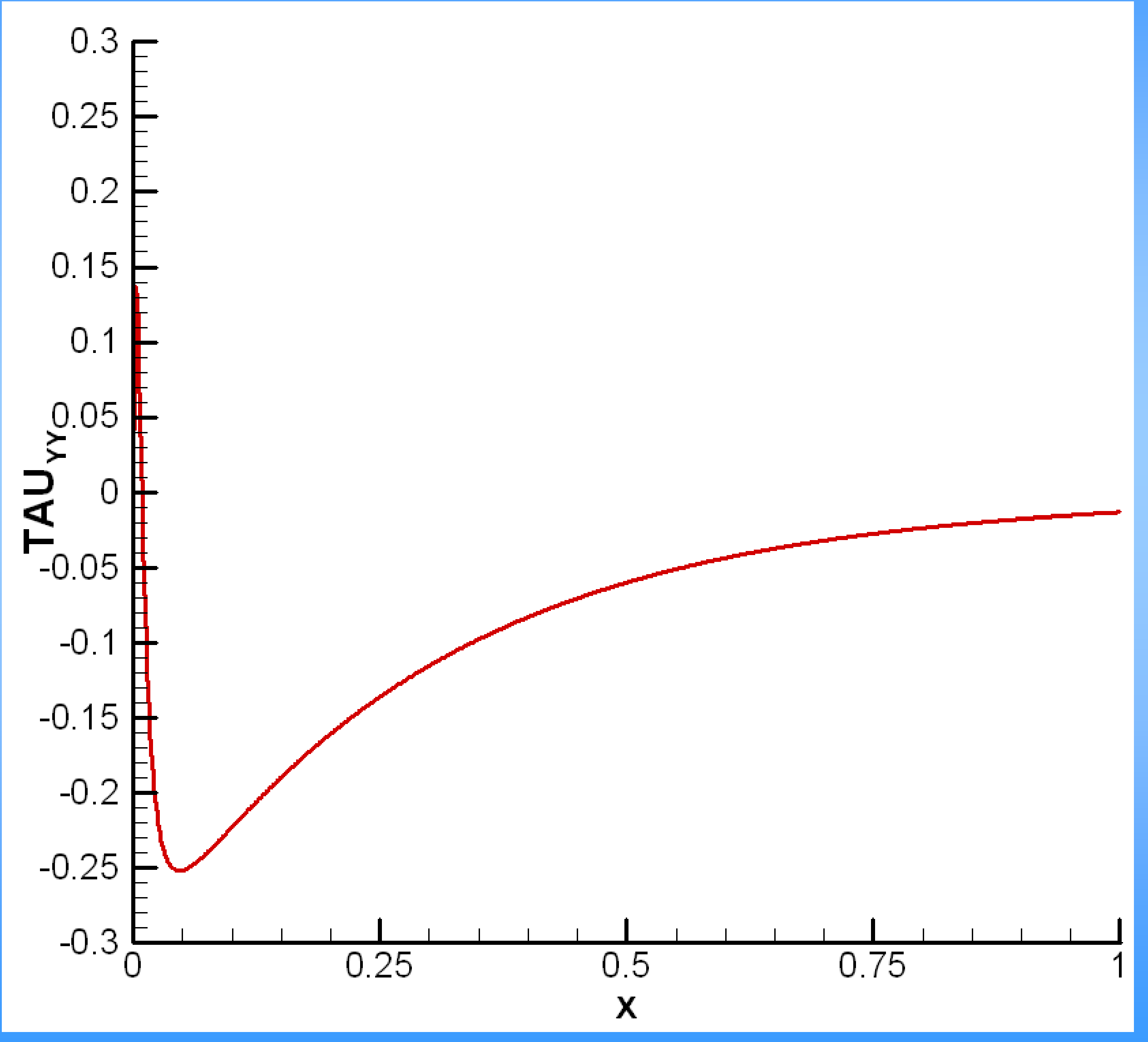

Unperturbed polymer jet in melt blowing: K(x) distribution

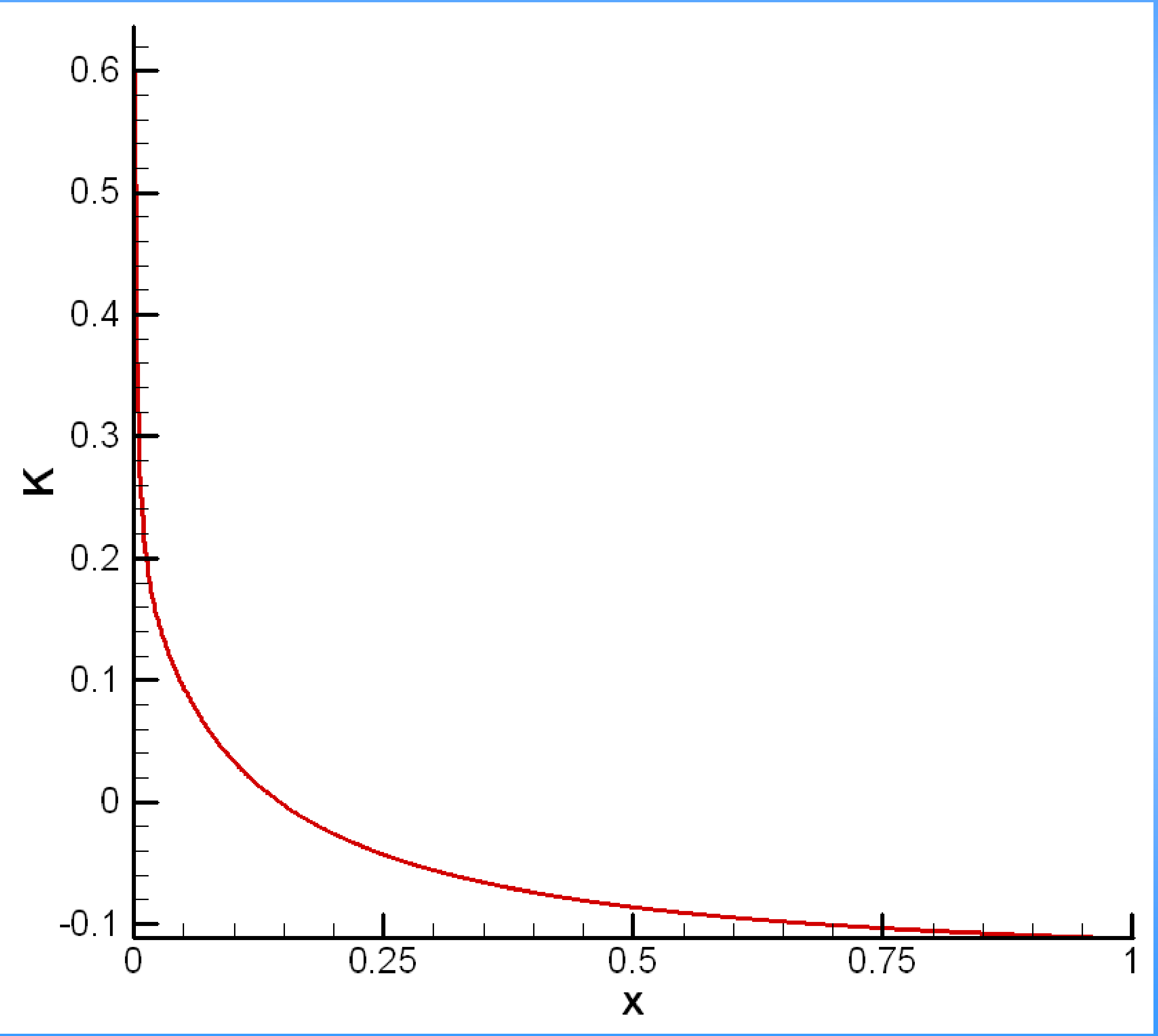

Bending perturbations of polymeric liquid jet in high speed air flow

The linearized lateral momentum balance

reads (dimensional):

$$\frac{\partial^2 H}{\partial t^2} + 2V_\tau \frac{\partial^2 H}{\partial x \partial t} + \left[V_\tau^2 + \frac{\rho_g (U_g - V_\tau)^2 - \sigma_{xx}}{\rho} \right] \frac{\partial^2 H}{\partial x^2} = 0$$

and normalized:

$$\frac{\partial^2 H}{\partial t^2} + 2V_\tau \frac{\partial^2 H}{\partial x \partial t} + \left[V_\tau^2 + R(U_g - V_\tau)^2 - E\sigma_{xx} \right] \frac{\partial^2 H}{\partial x^2} = 0$$

All coefficients depend only on the unperturbed solution!!!

Mechanical & Industrial Engineering

Bending perturbations of polymeric liquid jet in high speed air flow

Solution in the hyperbolic part:

$$H(x,t)=\frac{H_{0\omega}}{1-\delta}\exp(i\omega t)\begin{Bmatrix}-\delta\exp[-i\omega I_1(x)]\\+\exp[-i\omega I_2(x)]\end{Bmatrix}$$

where

$$I_1(x)=\int_0^x\frac{dx}{V_\tau(x)+\sqrt{E\sigma_{xx}(x)-R[U_g(x)-V_\tau(x)]^2}}$$

$$I_2(x)=\int_0^x\frac{dx}{V_\tau(x)-\sqrt{E\sigma_{xx}(x)-R[U_g(x)-V_\tau(x)]^2}}$$

$$\delta=\left.\frac{dI_2/dx}{dI_1/dx}\right|_{x=0}$$

Mechanical & Industrial Engineering

Bending perturbations of polymeric liquid jet in high speed air flow

Solution in the elliptic part :

$$H(x,t)=\frac{H_{0\omega}}{1-\delta}\exp\{i\omega[t-J_1(x)]\}$$
$$\times\left\{\begin{matrix}-\delta\exp[-i\omega I_1(x_*)]\exp[-\omega J_2(x)] \\ +\exp[-i\omega I_2(x_*)]\exp[\omega J_2(x)]\end{matrix}\right\}$$

where

$$J_1(x)=\int_{x*}^{x}\frac{V_\tau(x)}{V_\tau^2(x)+R[U_g(x)-V_\tau(x)]^2-E\sigma_{xx}(x)}dx$$

$$J_2(x)=\int_{x*}^{x}\frac{\sqrt{R[U_g(x)-V_\tau(x)]^2-E\sigma_{xx}(x)}}{V_\tau^2(x)+R[U_g(x)-V_\tau(x)]^2-E\sigma_{xx}(x)}dx$$

The velocity distribution in turbulent gas jet is

$$U_g(x)=U_g(0)\frac{2.4d_0}{x+2.4d_0}$$

Mechanical & Industrial Engineering

Bending perturbations of polymeric liquid jet in melt blowing

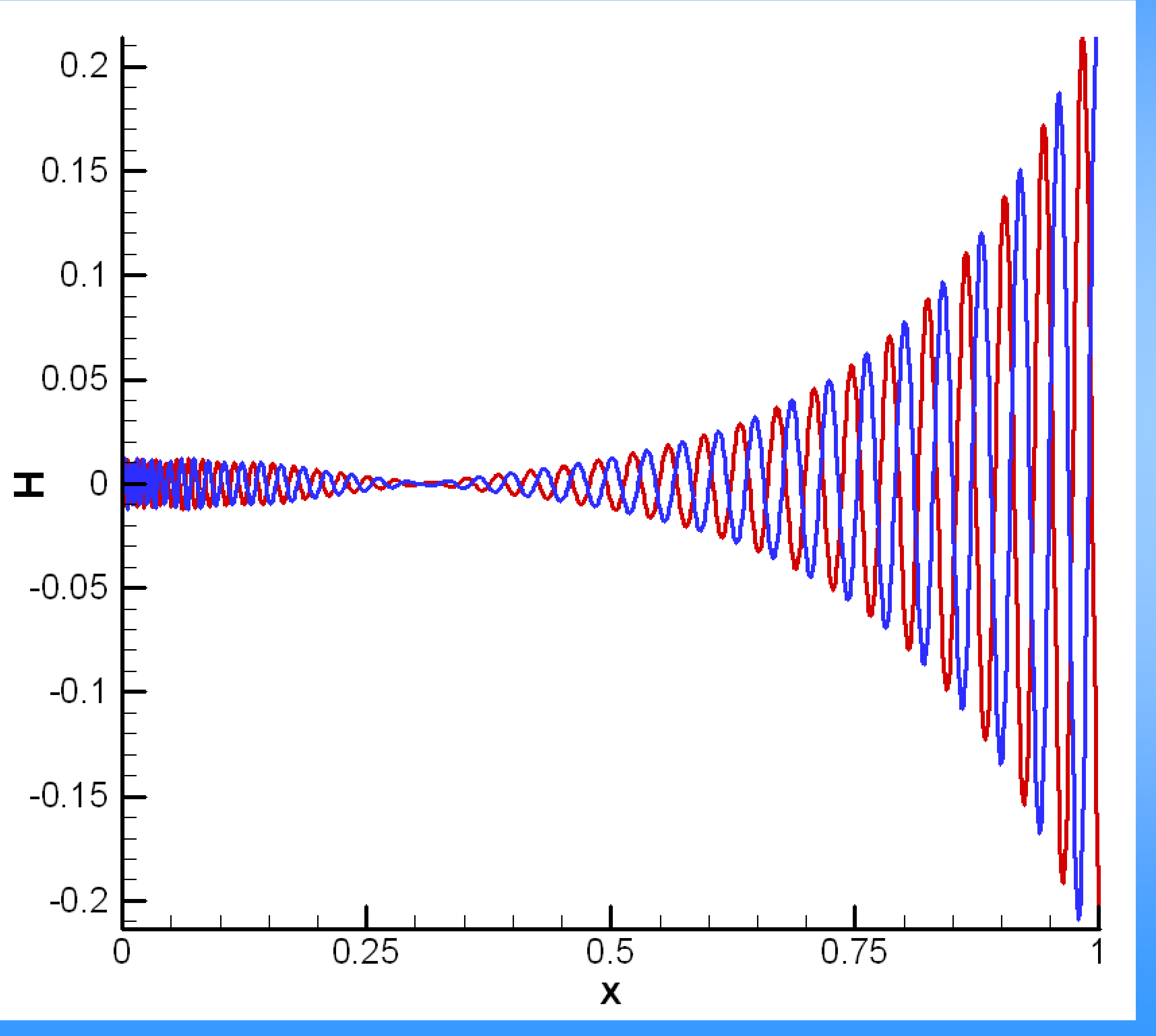

Meltblowing: Nonlinear theory

Nonlinear model for predicting large perturbations on polymeric viscoelastic jets.

- **Isothermal polymer and gas jets-2D bending of 1 jet**
  - Basic vectorial equations
  - Scalar projections of the momentum balance equation in 2D
  - Numerical results

- **Non-isothermal polymer and gas jets-2D bending of 1 jet**
  - Basic vectorial equations
  - Scalar projections of the momentum balance equation in 2D
  - Numerical results

- **3D results: single and multiple jets**

Mechanical & Industrial Engineering

A.L. Yarin, S. Sinha-Ray, B. Pourdeyhimi. J. Appl. Phys. 108, 034913 (2010).

Nonlinear Model for

Isothermal Polymer and Gas Jets

UIC Mechanical & Industrial Engineering

Basic equations: Momentless theory

$$\frac{\partial \lambda f}{\partial t} + \frac{\partial fW}{\partial s} = 0$$ ← Continuity Equation

$$\frac{\partial \lambda f \mathbf{V}}{\partial t} + \frac{\partial fW\mathbf{V}}{\partial s} = \frac{1}{\rho}\frac{\partial P\boldsymbol{\tau}}{\partial s} + \lambda f\mathbf{g} + \frac{\lambda}{\rho}\mathbf{q}_{total}$$ ← Momentum Equation

Taking s to be a Lagrangian parameter of liquid elements in the jet,

W=0, which gives $\lambda a^2 = \lambda_0 a_0^2$ - The integral of the continuity equation

Mechanical & Industrial Engineering

Relation of the coordinate system associated with the jet axis and the laboratory coordinate system in 2D cases

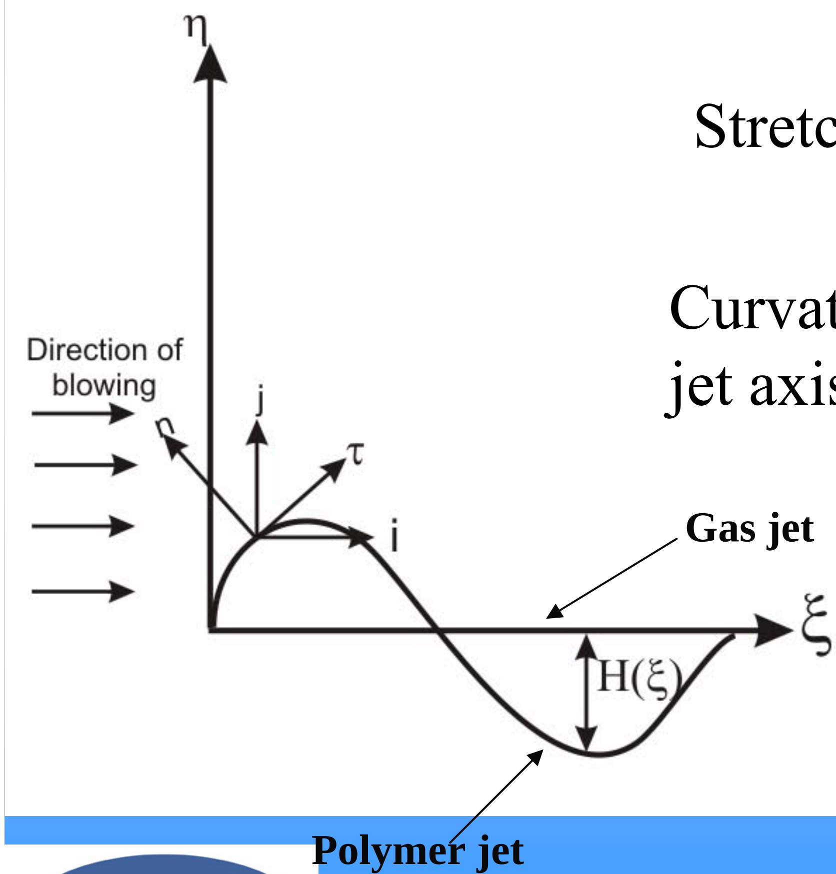

$$\mathbf{R} = \mathbf{i}\xi(s,t) + \mathbf{j}H(s,t)$$

Stretching ratio → $\lambda = \left(\xi_{,s}^{2} + H_{,s}^{2}\right)^{1/2}$

Curvature of the jet axis → $k = \dfrac{H_{,ss}\xi_{s} - \xi_{,ss}H_{,s}}{\left(\xi_{,s}^{2} + H_{,s}^{2}\right)^{3/2}}$

$$\tau_{\xi} = n_{\eta} = \left[1 + \left(H_{,s}/\xi_{,s}\right)^{2}\right]^{-1/2}$$

$$n_{\xi} = -\tau_{\eta} = -\left(H_{,s}/\xi_{,s}\right)\left[1 + \left(H_{,s}/\xi_{,s}\right)^{2}\right]^{-1/2}$$

Mechanical & Industrial Engineering

Scalar projections of the momentum balance equation in 2D

$$\frac{\partial V_\tau}{\partial t} = V_n\left(\frac{1}{\lambda}\frac{\partial V_n}{\partial s} + kV_\tau\right) + \frac{1}{\rho f \lambda}\frac{\partial P}{\partial s} + g_\tau + \frac{q_{total,\tau}}{\rho f}$$

$$\frac{\partial V_n}{\partial t} = -V_\tau\left(\frac{1}{\lambda}\frac{\partial V_n}{\partial s} + kV_\tau\right) + \frac{Pk}{\rho f} + g_n + \frac{q_{total,n}}{\rho f}$$

$$\mathbf{q}_{total} = \mathbf{n} q_{total,n} + \boldsymbol{\tau} q_{total,\tau} =$$

$$-\rho_g U_g^2 \mathbf{n}\left[f\frac{\xi_{,s}^2\left(H_{,ss}\xi_{,s} - \xi_{,ss}H_{,s}\right)}{\left(\xi_{,s}^2 + H_{,s}^2\right)^{5/2}} + a\frac{\left(H_{,s}/\xi_{,s}\right)^2 \operatorname{sign}\left(H_{,s}/\xi_{,s}\right)}{1+\left(H_{,s}/\xi_{,s}\right)^2}\right]$$

$$+\pi a \rho_g\left(U_g \tau_\xi - V_\tau\right)^2 0.65\left[\frac{2a\left(U_g\tau_\xi - V_\tau\right)}{\nu_g}\right]^{-0.81}\boldsymbol{\tau}$$

Mechanical & Industrial Engineering

The rheological constitutive viscoelastic model. The mean flow field in the turbulent gas jet

Rheological Constitutive Equation :Upper Convected Maxwell Model

$$\frac{\partial \tau_{\tau\tau}}{\partial t} = 2\tau_{\tau\tau}\frac{1}{\lambda}\frac{\partial \lambda}{\partial t} + 2\frac{\mu}{\theta}\frac{1}{\lambda}\frac{\partial \lambda}{\partial t} - \frac{\tau_{\tau\tau}}{\theta}$$

The mean flow field in the turbulent gas jet

$$U_g(\xi, H) = U_{g0}\varphi(\xi, H)$$

$$\varphi(\xi, H) = \frac{4.8/\ell}{\left(\xi + 4.8/\ell\right)}\frac{1}{\left(1+\varsigma^2/8\right)^2}, \quad \varsigma = \varsigma(\xi, H) = \frac{H}{0.05\left(\xi + 4.8/\ell\right)}$$

L/a_0, where a_0 is the nozzle radius and L is the distance between the nozzle and deposition screen

Mechanical & Industrial Engineering

Dimensionless groups

Time, co-ordinates and functions	Rendered dimensionless by the scales
t	L/U_{g0}
s, H, ξ	L
k	L^{-1}
$\tau_{\tau\tau}$	$\mu U_{g0}/L$
U_{g0}, U_g, V_τ, V_n	U_{g0}
a	a_0
$q_{total,\tau}$	$\rho_g U_{g0}^2 a_0$
ν_t	μ/ρ

$$\mathrm{Re} = \frac{\rho L U_{g0}}{\mu}$$

$$J = \frac{\rho_g}{\rho}$$

$$\mathrm{Fr} = \left[\frac{U_{g0}^2}{gL}\right]^{1/2}$$

$$\mathrm{Re}_a = \frac{2a_0 U_{g0}}{\nu_g}$$

$$\mathrm{De} = \frac{\theta U_{g0}}{L}$$

Mechanical & Industrial Engineering

Dimensionless equations for numerical implementation

$$\frac{\partial^2 \xi}{\partial t^2} = \frac{2}{\mathrm{Re}} \Phi \frac{\partial^2 \xi}{\partial s^2} + \frac{1}{\mathrm{Fr}^2} \tau_\xi + J\ell \frac{q_{\mathrm{total},\tau}}{f} \qquad (1)$$

$$\frac{\partial^2 H}{\partial t^2} = \left[\frac{\tau_{\tau\tau}}{\mathrm{Re}} - J\varphi^2(\xi,H)\right] \frac{1}{\lambda^2} \frac{\partial^2 H}{\partial s^2} + \frac{n_\xi}{\mathrm{Fr}^2} - J\ell \frac{\varphi^2(\xi,H)}{\pi a} \frac{\left(H_{,s}/\xi_{,s}\right)^2 \mathrm{sign}\left(H_{,s}/\xi_{,s}\right)}{1+\left(H_{,s}/\xi_{,s}\right)^2} \qquad (2)$$

where $\Phi = \left(\tau_{\tau\tau} + 1/\mathrm{De}\right)\lambda^{-2}$, and Φ is found from: $\dfrac{\partial \Phi}{\partial t} = -\dfrac{\tau_{\tau\tau}}{\mathrm{De}\lambda^2}$ (3)

and $q_{\mathrm{total},\tau} = \pi a \left[\tau_\xi \varphi(\xi,H) - V_\tau\right]^2 0.65 \left\{\mathrm{Re}_a\, a\left[\tau_\xi \varphi(\xi,H) - V_\tau\right]\right\}^{-0.81}$

Mechanical & Industrial Engineering

Nature of the equations

$$\frac{\partial^2 \xi}{\partial t^2} = \frac{2}{Re}\Phi\frac{\partial^2 \xi}{\partial s^2} + \frac{1}{Fr^2}\tau_\xi + J\ell\frac{q_{total,\tau}}{f} \qquad (1)$$

$$\frac{\partial^2 H}{\partial t^2} = \left[\frac{\tau_{\tau\tau}}{Re} - J\varphi^2(\xi,H)\right]\frac{1}{\lambda^2}\frac{\partial^2 H}{\partial s^2} + \frac{n_\xi}{Fr^2} - J\ell\frac{\varphi^2(\xi,H)}{\pi a}\frac{\left(H_{,s}/\xi_{,s}\right)^2 \operatorname{sign}\left(H_{,s}/\xi_{,s}\right)}{1+\left(H_{,s}/\xi_{,s}\right)^2} \qquad (2)$$

Both the equations are basically wave equations. While (1) is –for the elastic sound (compression/stretching) wave propagation, (2) is nothing but bending wave propagation.

Mechanical & Industrial Engineering

Boundary and initial conditions

Boundary Conditions:

1) $\xi\big|_{s=s_{origin}} = 0, \quad H\big|_{s=s_{origin}} = H_{0\Omega}\exp(i\Omega t)$

where $H_{0\Omega} = \left(0.06/\ell\right)^{1/2}\mathrm{Re}^{1/2}/\tau_{\tau\tau 0}^{1/4} \qquad \Omega = \dfrac{\omega L}{U_{g0}}$

2) $\xi_{,s}\big|_{s_{\text{free end}}} = 1, \qquad H_{,s}\big|_{s_{\text{free end}}} = 0$

The initial condition for the longitudinal stress in the polymer jet:

$$\Phi\big|_{t=t_{birth}} = \left(\tau_{\tau\tau 0} + 1/De\right)/\lambda_0^2$$

Mechanical & Industrial Engineering

Numerical results for 2D: the isothermal case

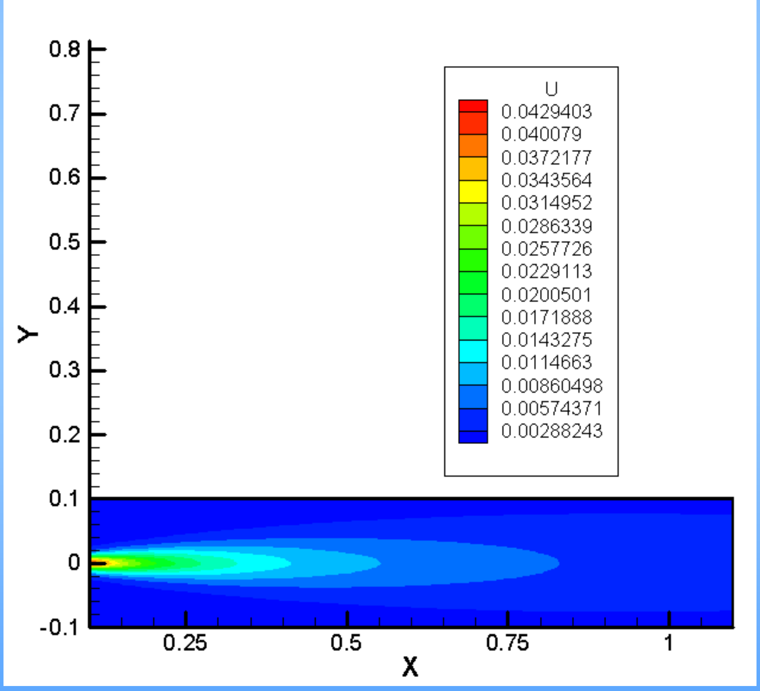

Velocity flow field in gas jet

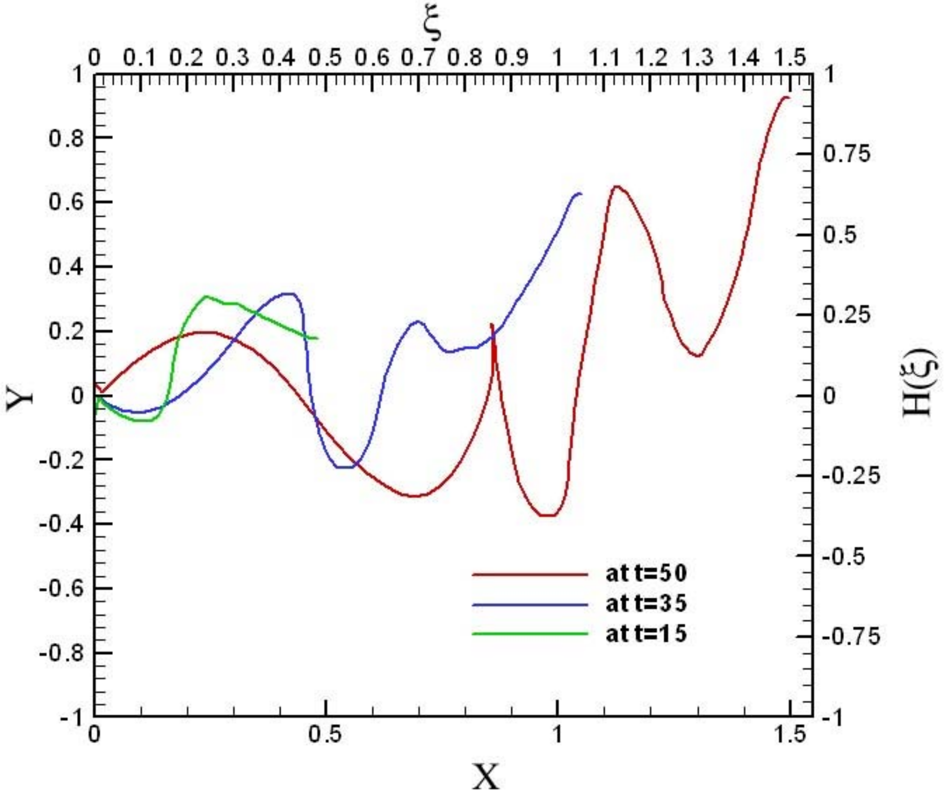

Snapshots of configurations of polymer jet axis

Mechanical & Industrial Engineering

Numerical results in 2D: the isothermal case (continued)

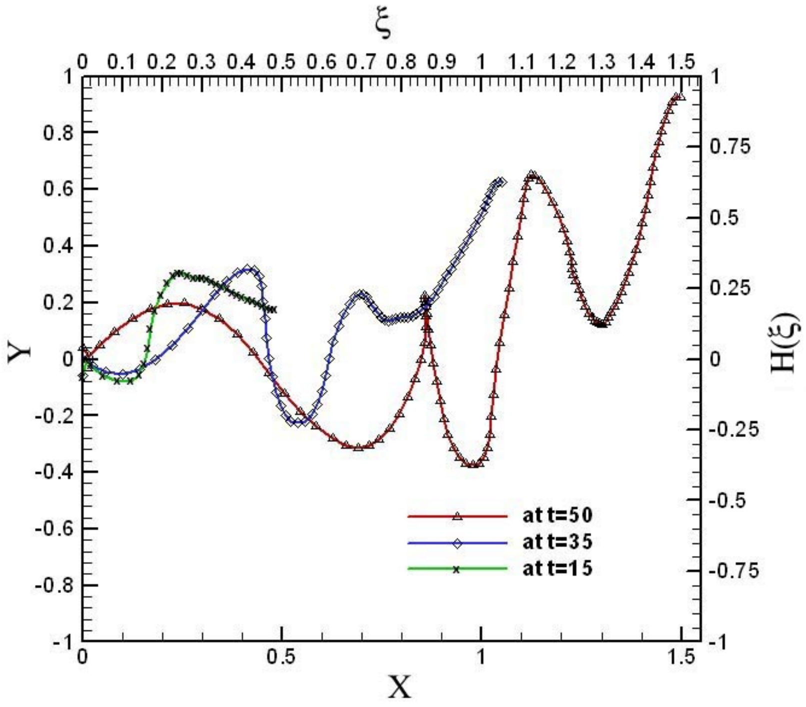

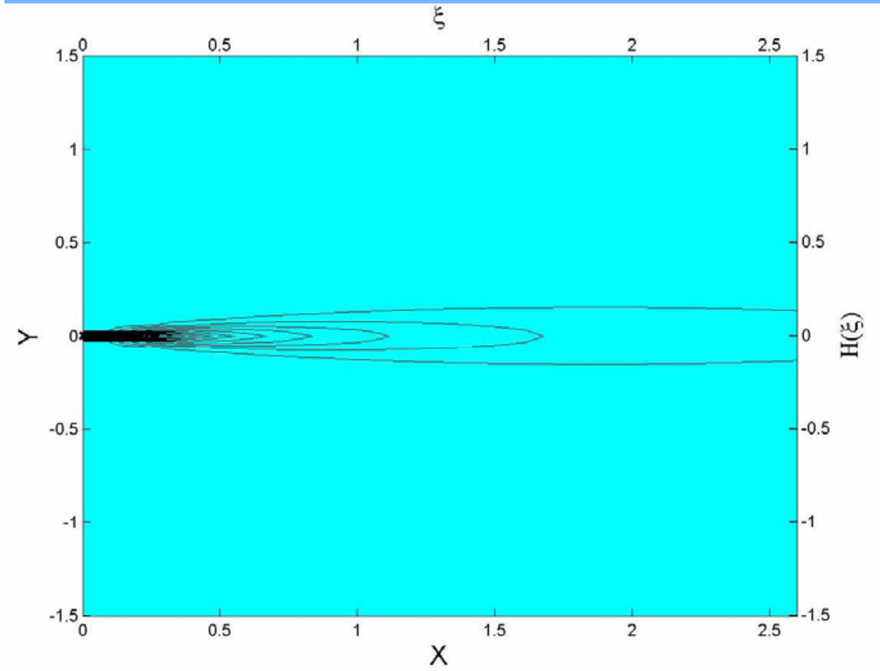

Self-entanglement: Can lead to "roping" and "fly"

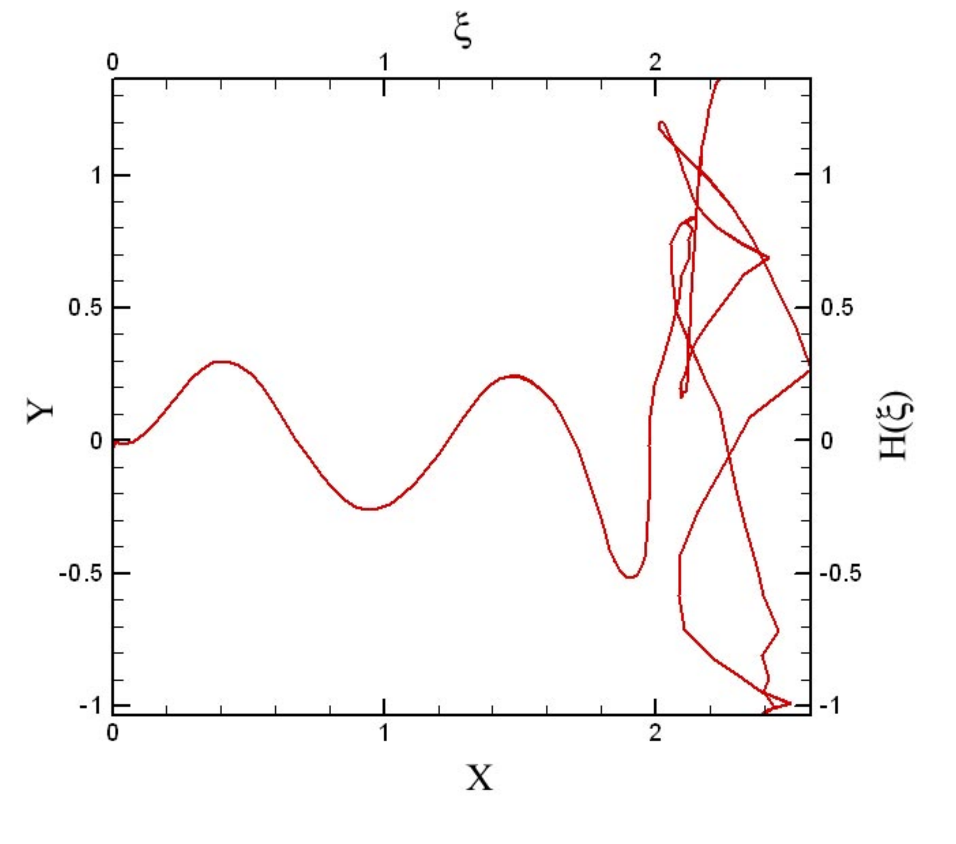

The evolution points at possible self-intersection in meltblowing, even in the case of a single jet considered here

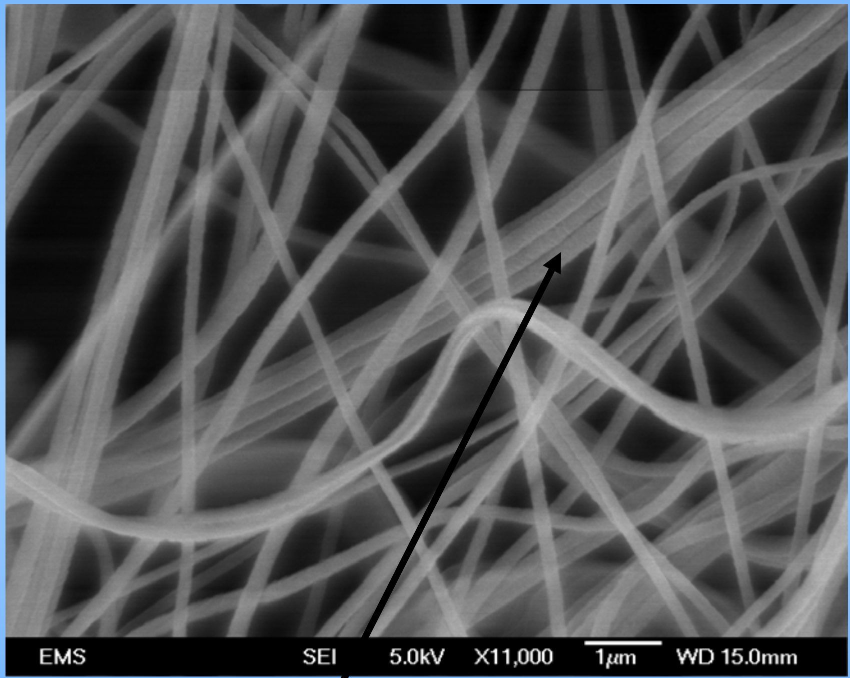

SEM image of solution blown PAN fiber mat obtained from single jet showing existence of "roping"

Mechanical & Industrial Engineering

Nonlinear Model for

Non-isothermal Polymer and Gas Jets

Mechanical & Industrial Engineering

Thermal variation of the rheological parameters

$$\mu = \mu_0 \exp\left[\frac{U}{R}\left(\frac{1}{T} - \frac{1}{T_0}\right)\right], \quad \theta = \theta_0 \frac{T_0}{T} \exp\left[\frac{U}{R}\left(\frac{1}{T} - \frac{1}{T_0}\right)\right]$$

where T_0 is the melt and gas jet temperature at the origin, μ_0 and θ_0 are the corresponding values of the viscosity and relaxation time, U is the activation energy of viscous flow and R is the absolute gas constant.

The additional and changed dimensionless equations; 2D, non-isothermal case

$$\frac{\partial T}{\partial t} = -2\mathrm{Nu}\ell \frac{JC}{\mathrm{Re}_a \, \mathrm{Pr}_g} \frac{\lambda}{\lambda_0}\left(T - T_g\right)$$ ← Thermal Balance Equation

$$\frac{\partial \Phi}{\partial t} = -\frac{2\mathrm{Nu}\ell JC}{\mathrm{Re}_a \, \mathrm{Pr}_g \, \mathrm{De}_0 \lambda_0} \frac{\left(T - T_g\right)}{\lambda} - T\exp\left[-U_A\left(\frac{1}{T} - 1\right)\right]\frac{\tau_{\tau\tau}}{\mathrm{De}_0 \lambda^2}$$ ← Rheological Constitutive Equation

$$T_g(\xi, H) = T_{g\infty} + \frac{\left(\mathrm{Pr}_t + 1/2\right)}{0.05\sqrt{6}} \frac{\left(1 - T_{g\infty}\right)}{\ell} \frac{1}{\left(\xi + 4.8/\ell\right)} \frac{1}{\left(1 + \varsigma^2/8\right)^{2\mathrm{Pr}_t}}$$ ← Mean Temperature Field in the Gas Jet

where

$$\Phi = \left(\tau_{\tau\tau} + T/\mathrm{De}_0\right)/\lambda^2; \quad \mathrm{De}_0 = \frac{\theta_0 U_{go}}{L}, \quad U_A = \frac{U}{RT_0}, \qquad \mathrm{Nu} = 0.495\,\mathrm{Re}_a^{1/3}\,\mathrm{Pr}_g^{1/3}$$

Mechanical & Industrial Engineering

Numerical results for the 2D non-isothermal case

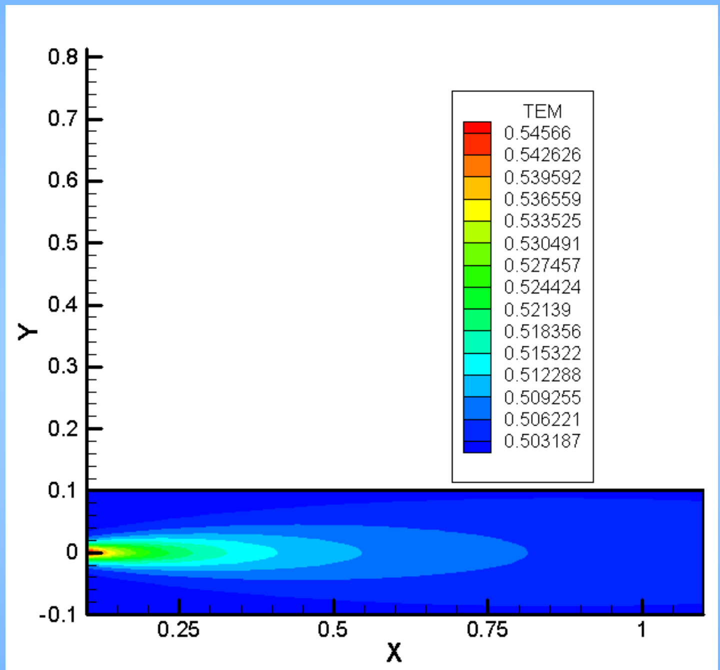

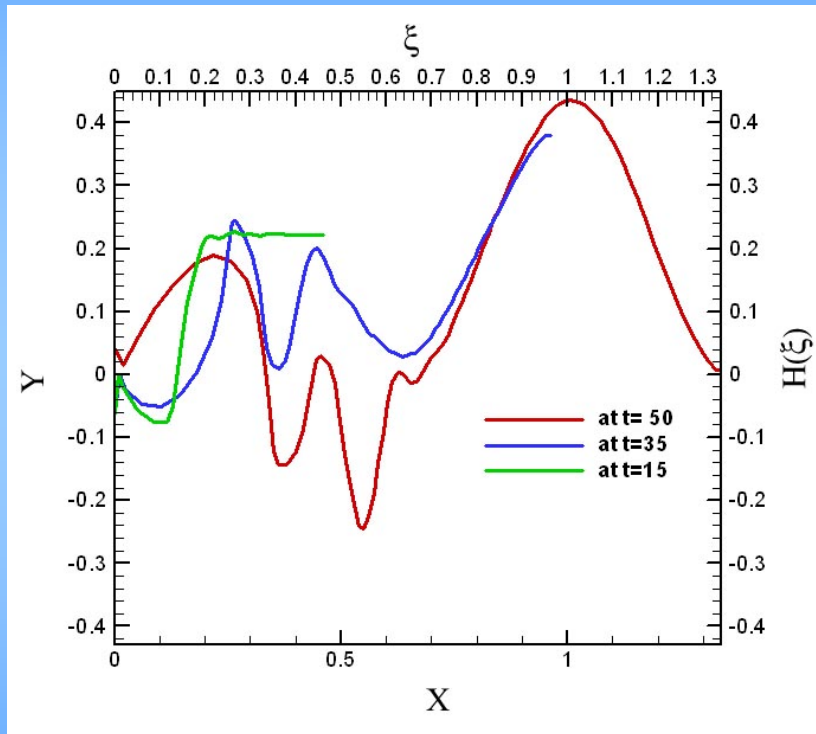

Snapshots of the axis configurations of polymer jet for the nonisothermal case

The mean temperature field in the gas jet

Mechanical & Industrial Engineering

Numerical results for the 2D non-isothermal case

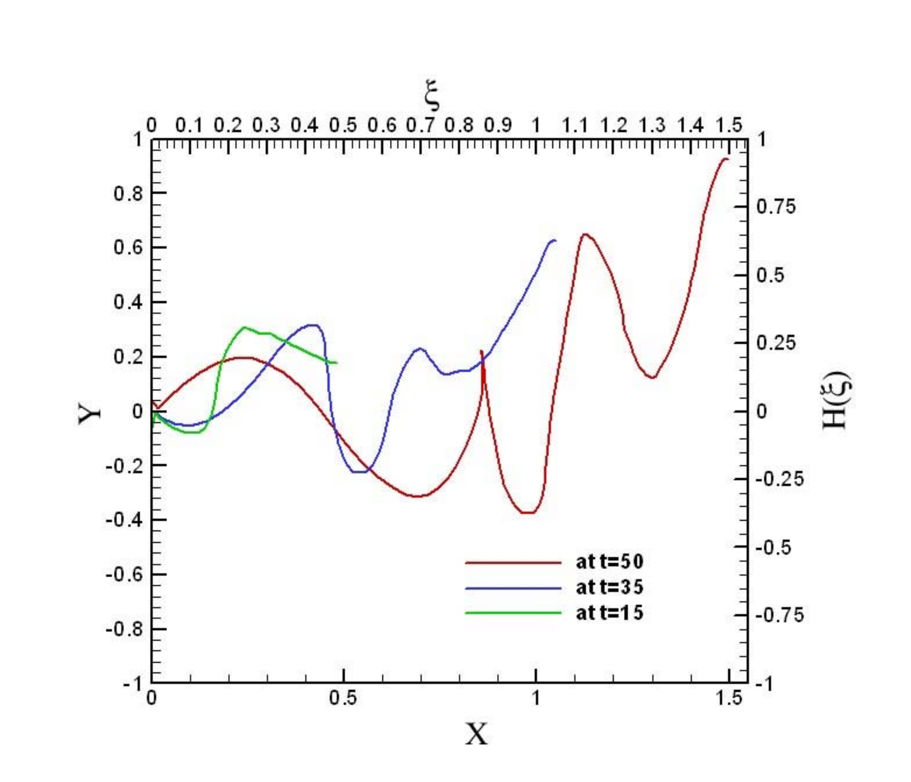

Snapshots of the axis configurations of the polymer jet in the isothermal case

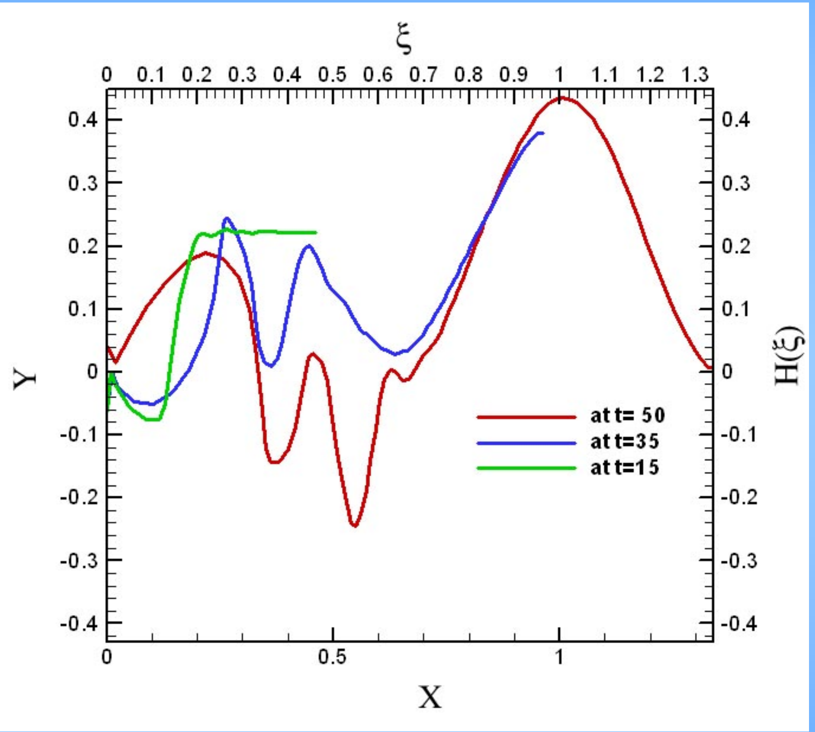

Snapshots of the axis configurations of the polymer jet for the nonisothermal case

Numerical results (continued)

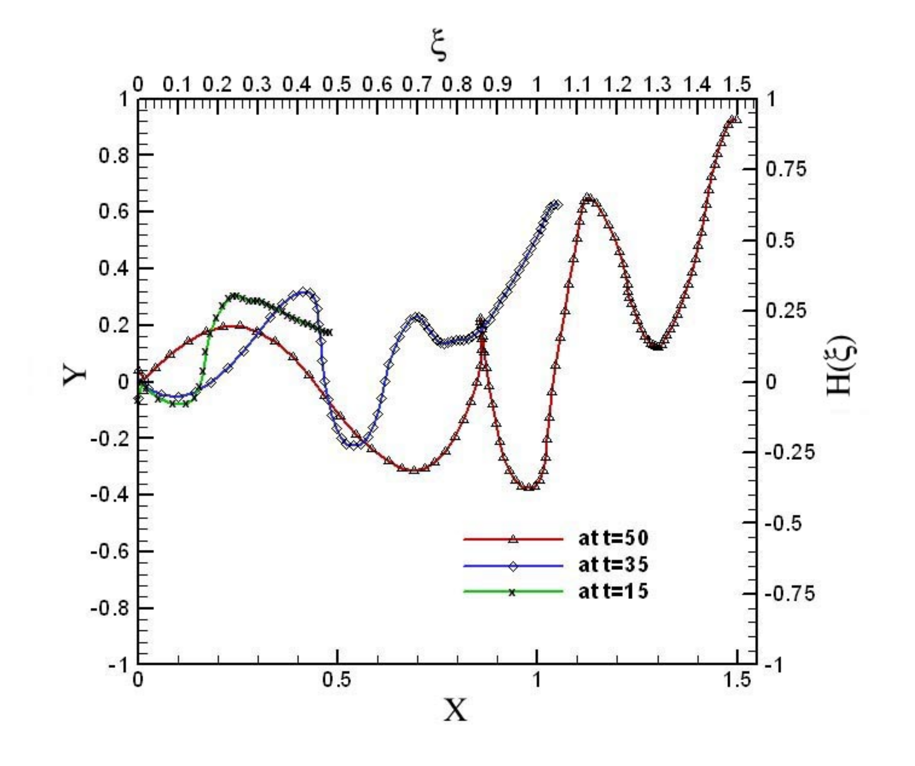

Following material elements in the polymer jet in the isothermal case

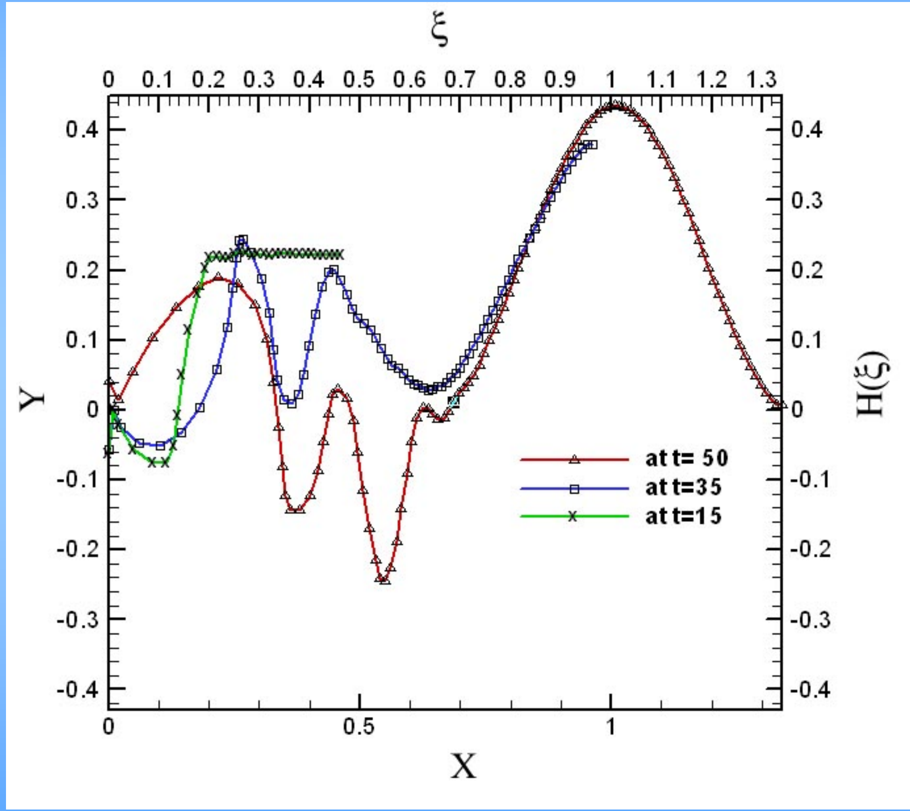

Following material elements in the polymer jet in the non-isothermal case

Mechanical & Industrial Engineering

The initial section of the jet-no bending

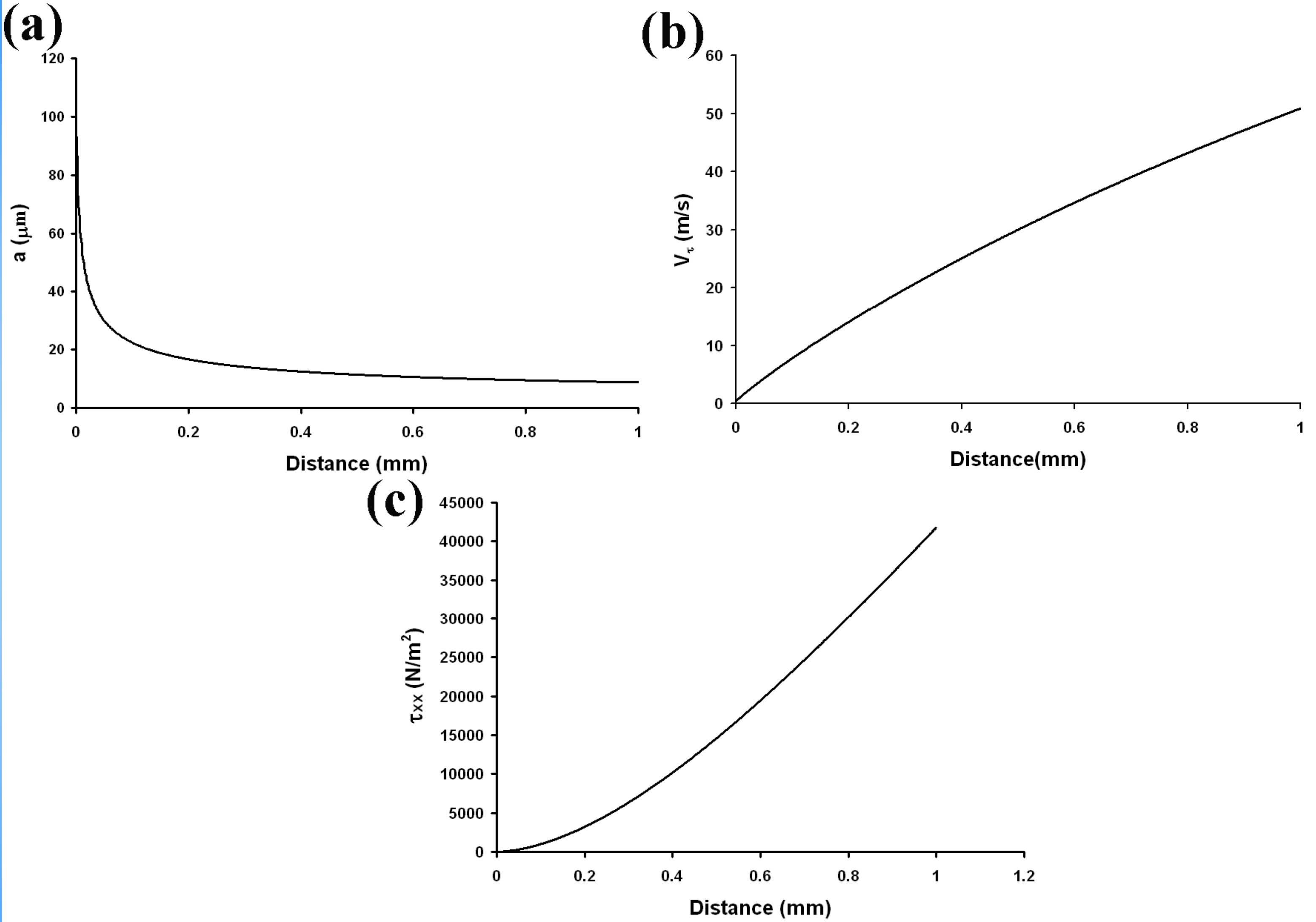

Mechanical & Industrial Engineering

3D isothermal results: single jet

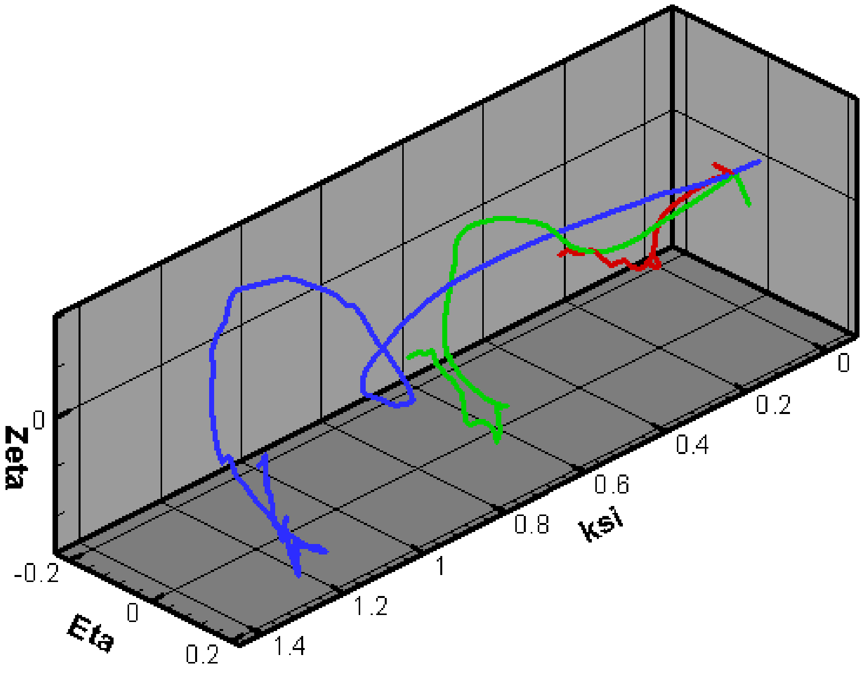

Three snapshots of the polymer jet axis in the isothermal three-dimensional blowing at the dimensional time moments t=15, 30 and 45

Mechanical & Industrial Engineering

9 jets meltblown onto a moving screen-the beginning of deposition

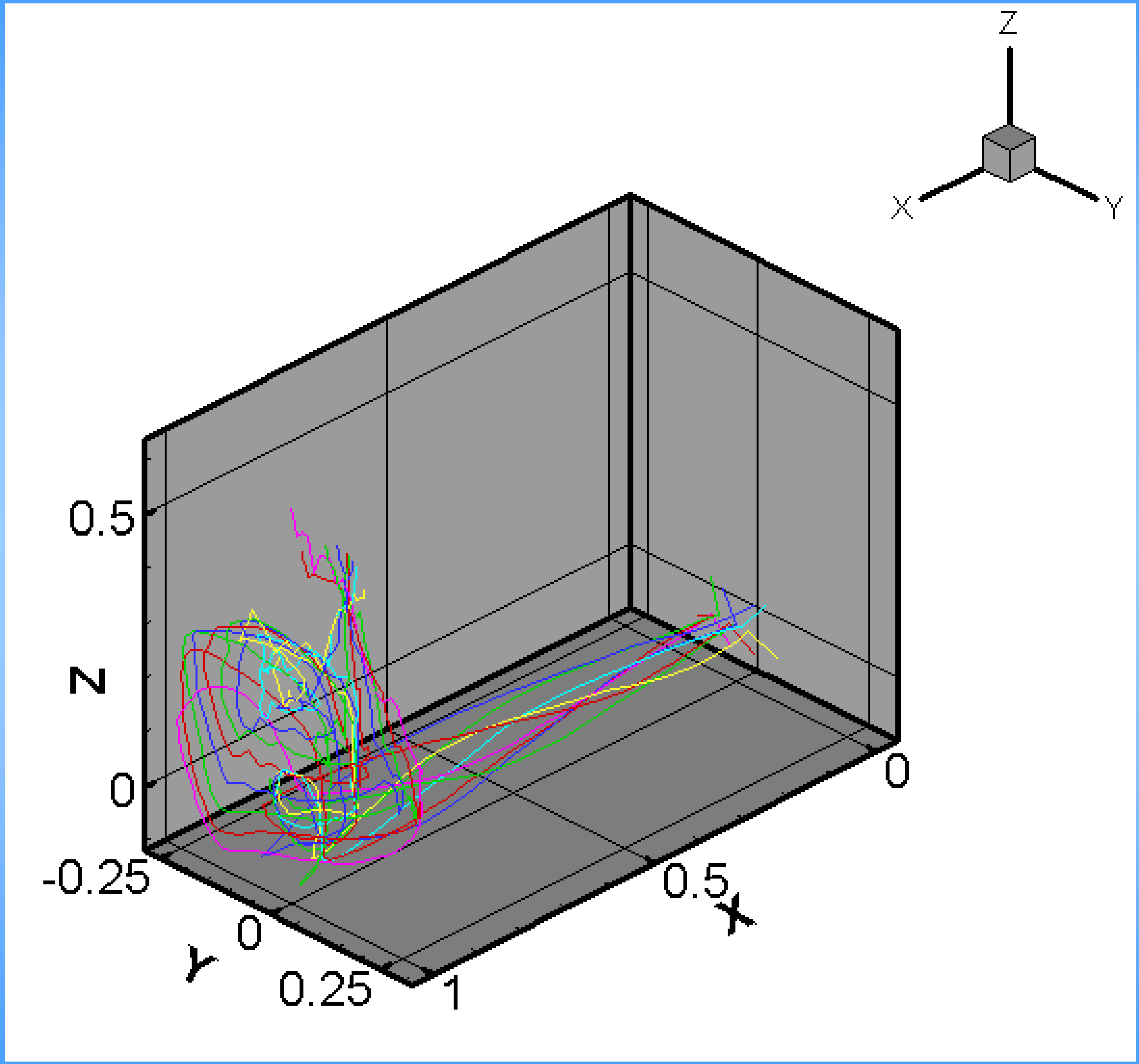

Mechanical & Industrial Engineering

9 jets meltblown onto a moving screen-a later moment

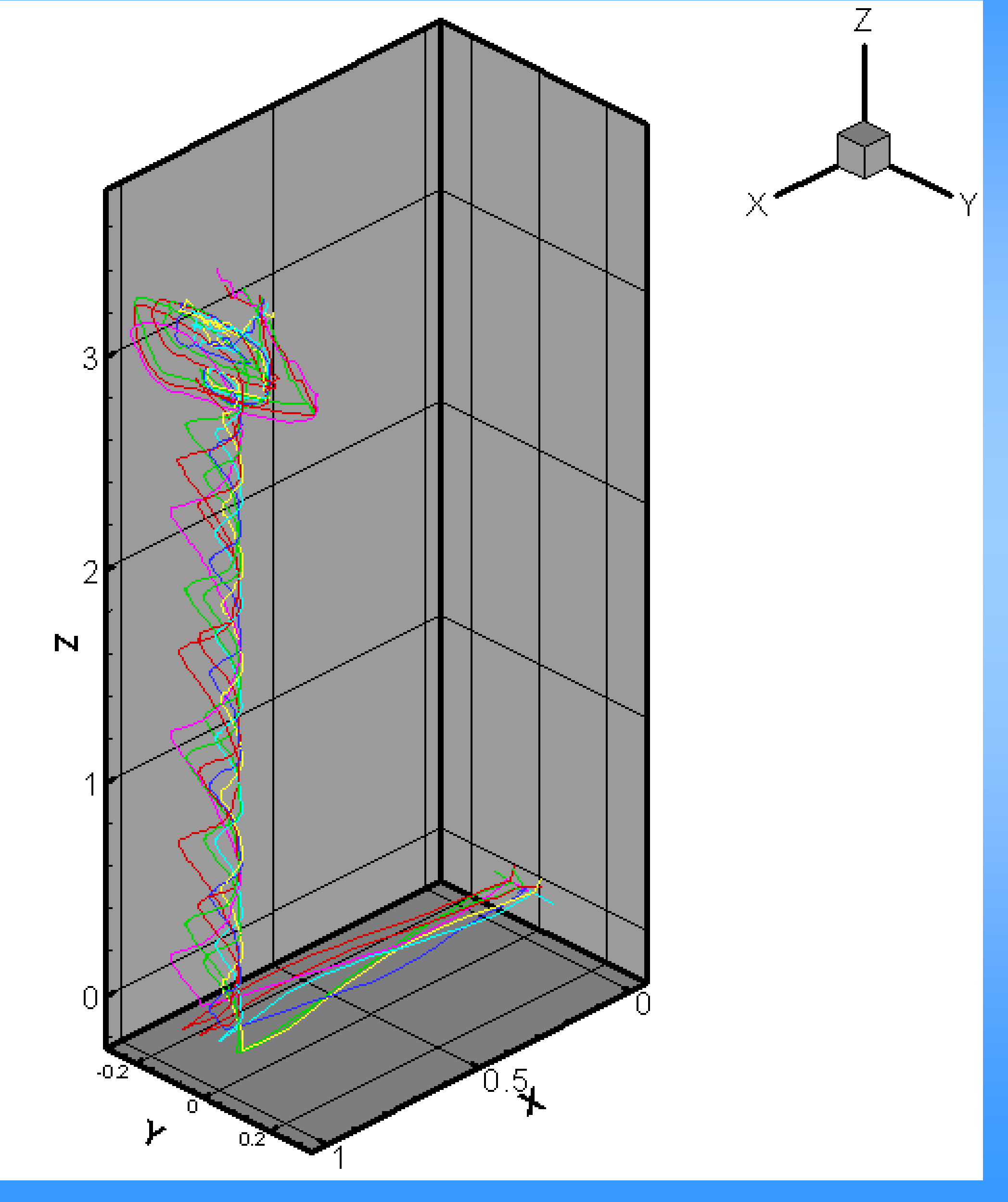

62 jets meltblown onto a moving screen

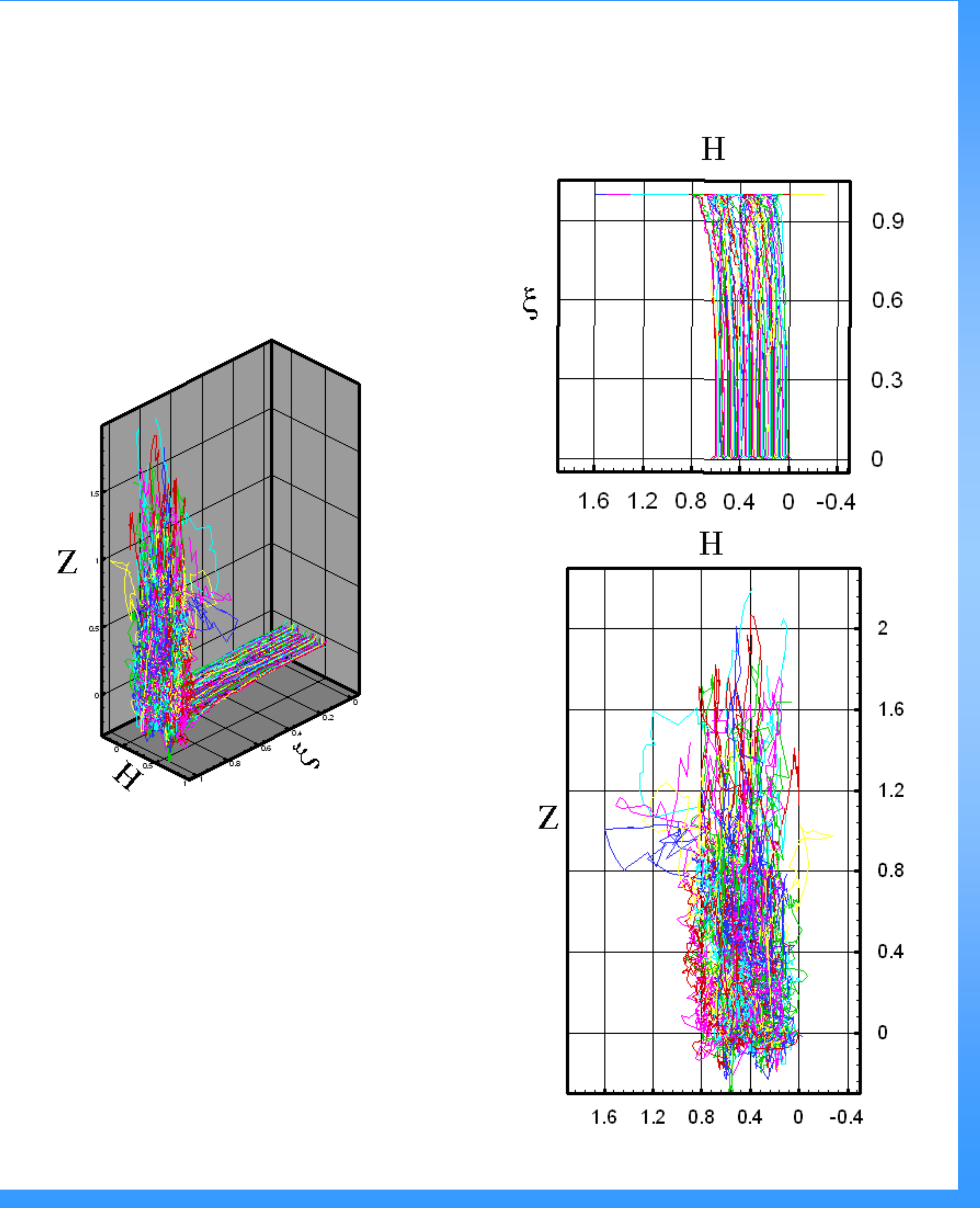

Mechanical & Industrial Engineering

62 jets meltblown onto a moving screen

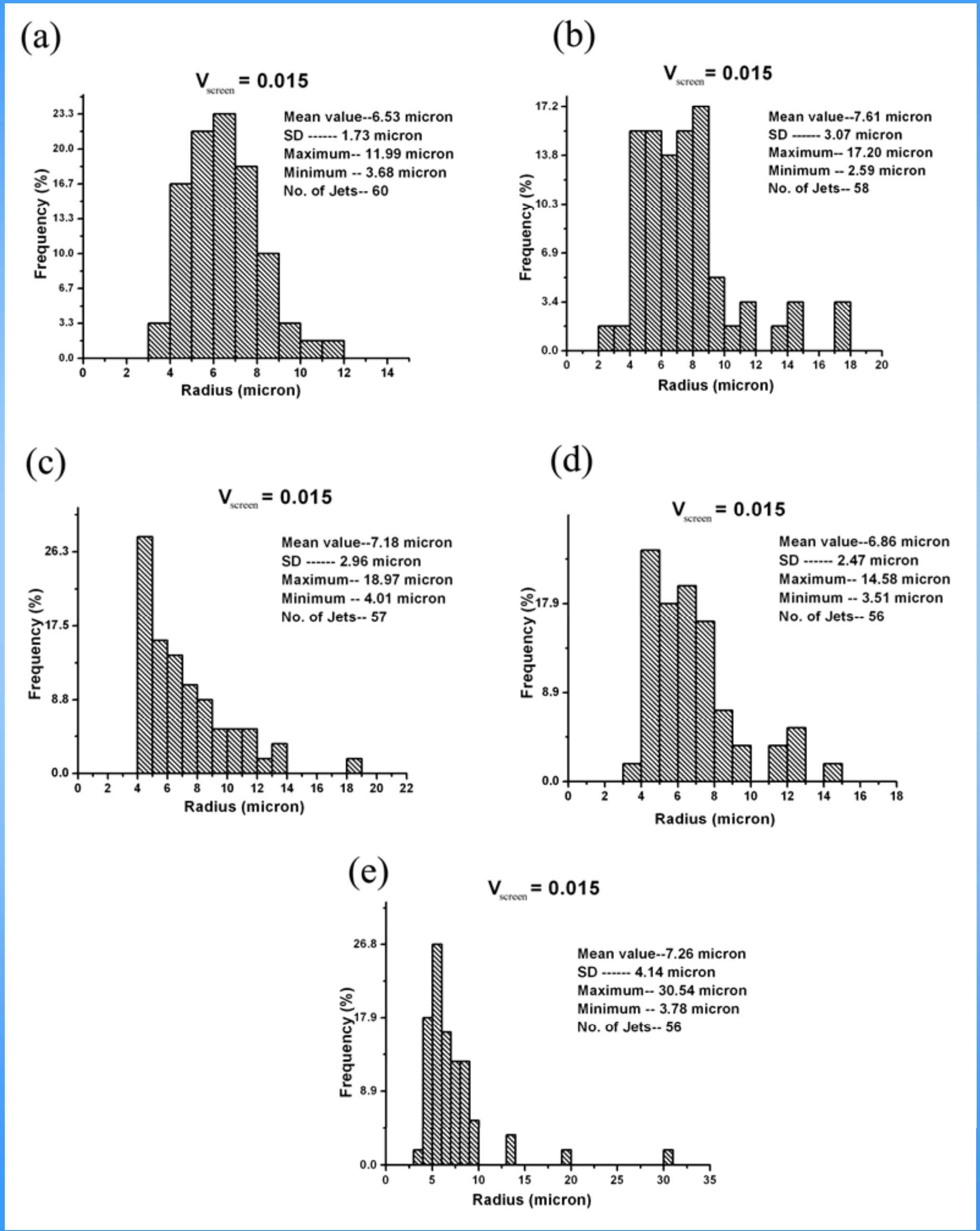

Mechanical & Industrial Engineering

62 jets meltblown onto a moving screen: a higher screen velocity

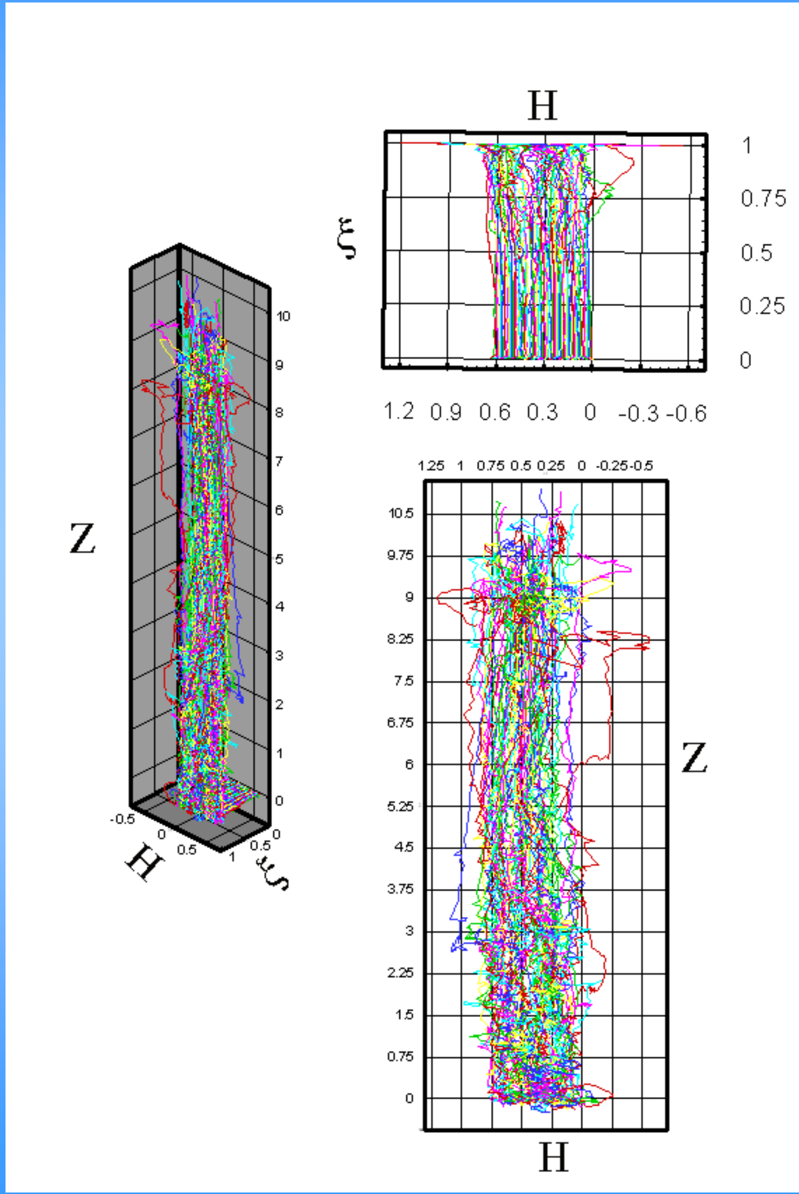

Mechanical & Industrial Engineering

62 jets meltblown onto a moving screen: a higher screen velocity

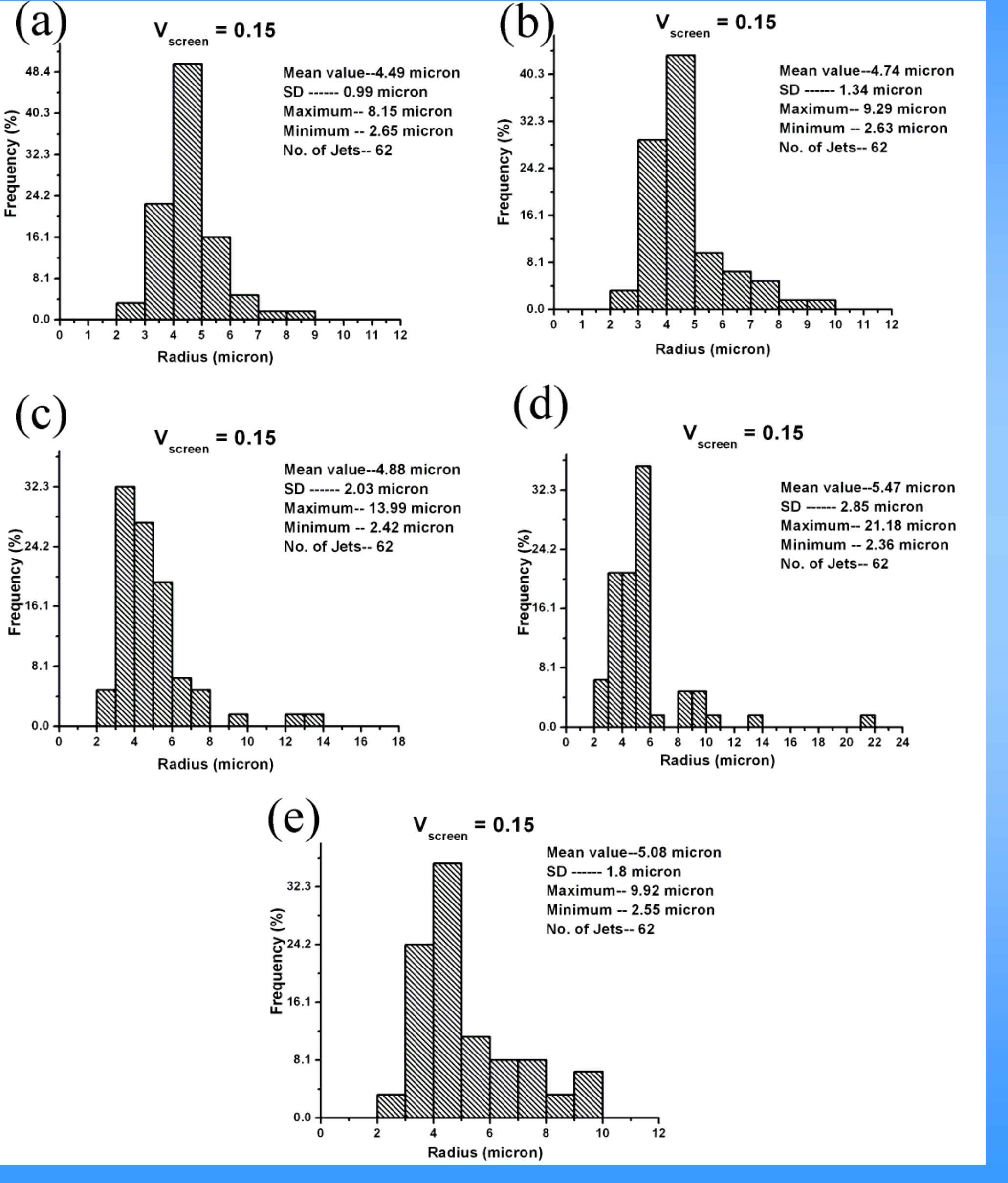

62 jets meltblown onto a moving screen: comparison with experiment

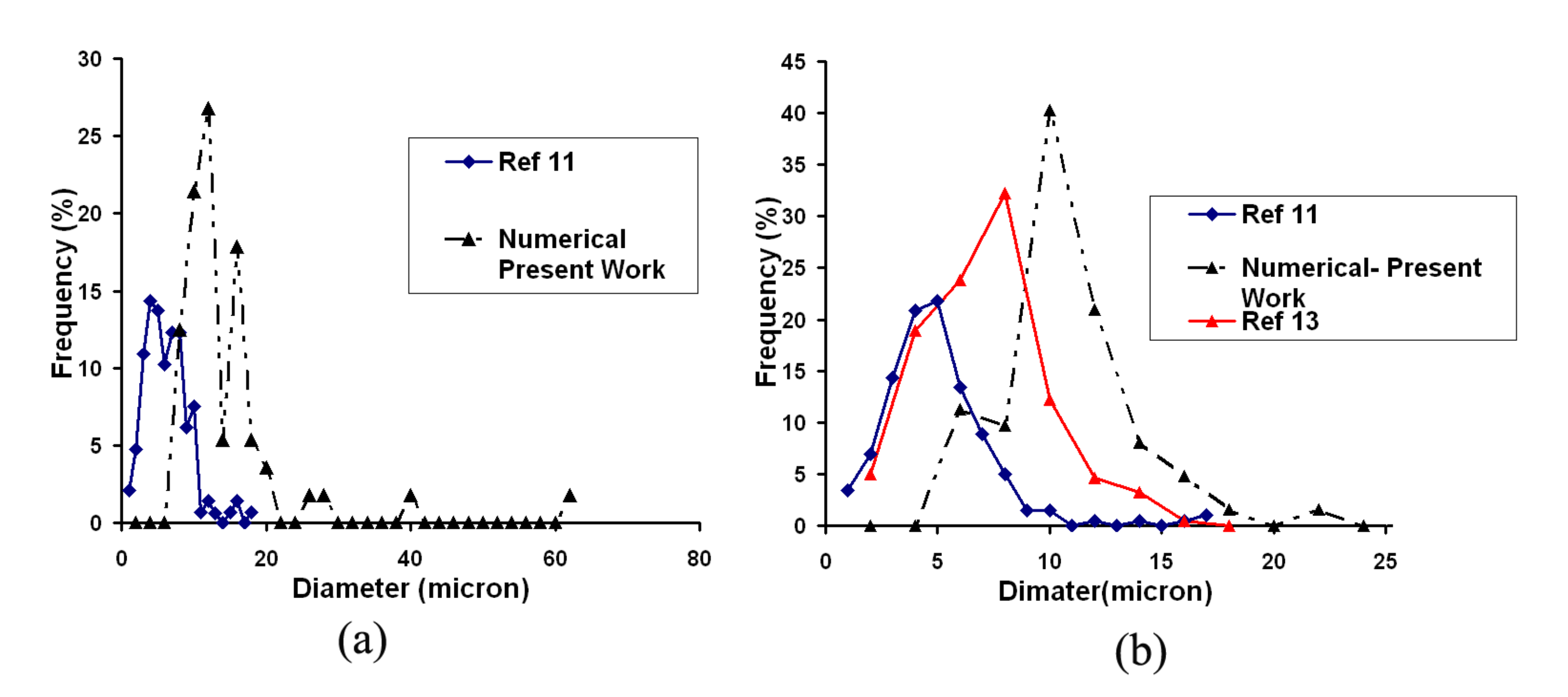

Mechanical & Industrial Engineering

62 jets meltblown onto a moving screen: comparison with experiment

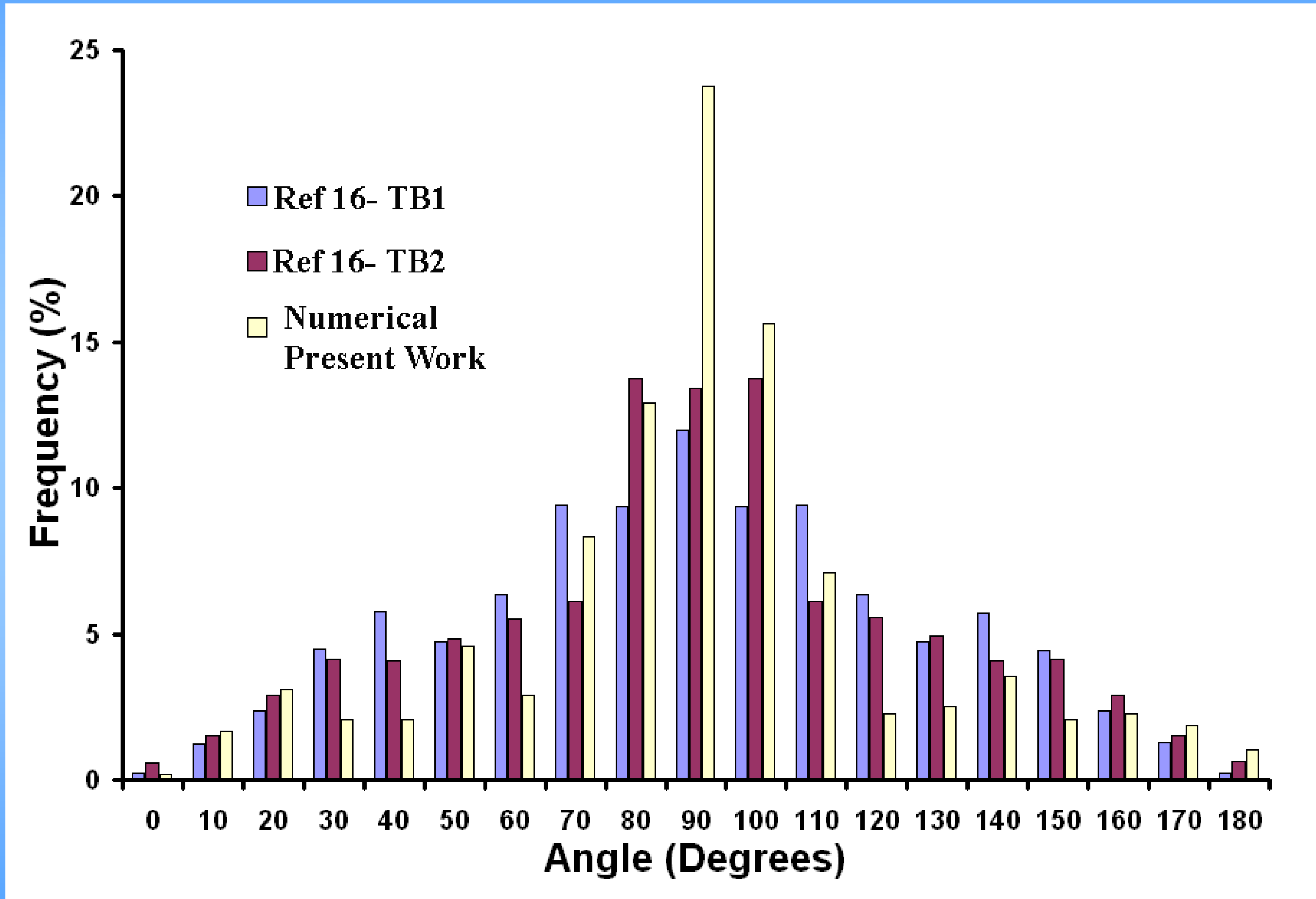

Mechanical & Industrial Engineering

62 jets meltblown onto a moving screen

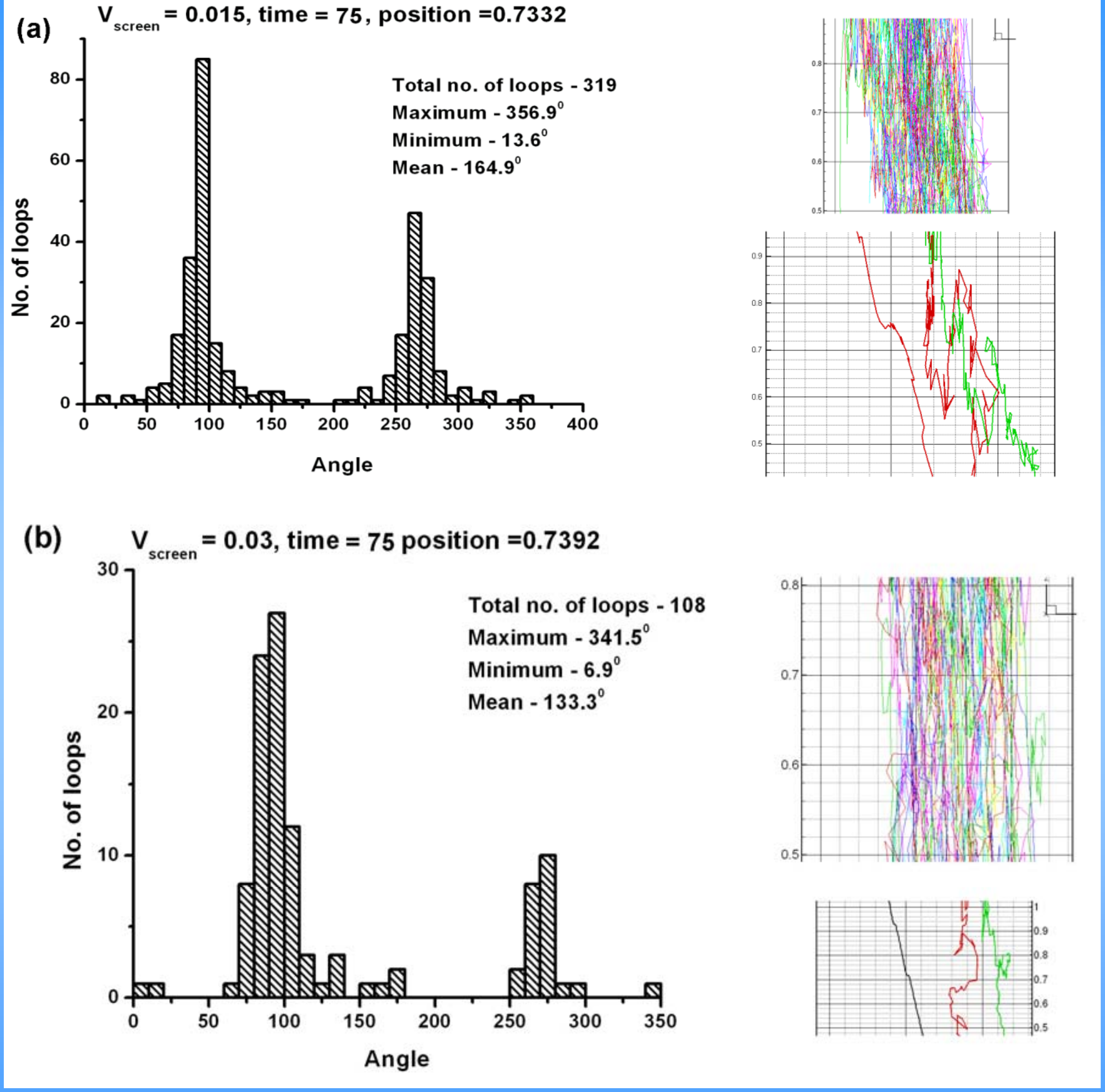

Mechanical & Industrial Engineering

62 jets meltblown onto a moving screen

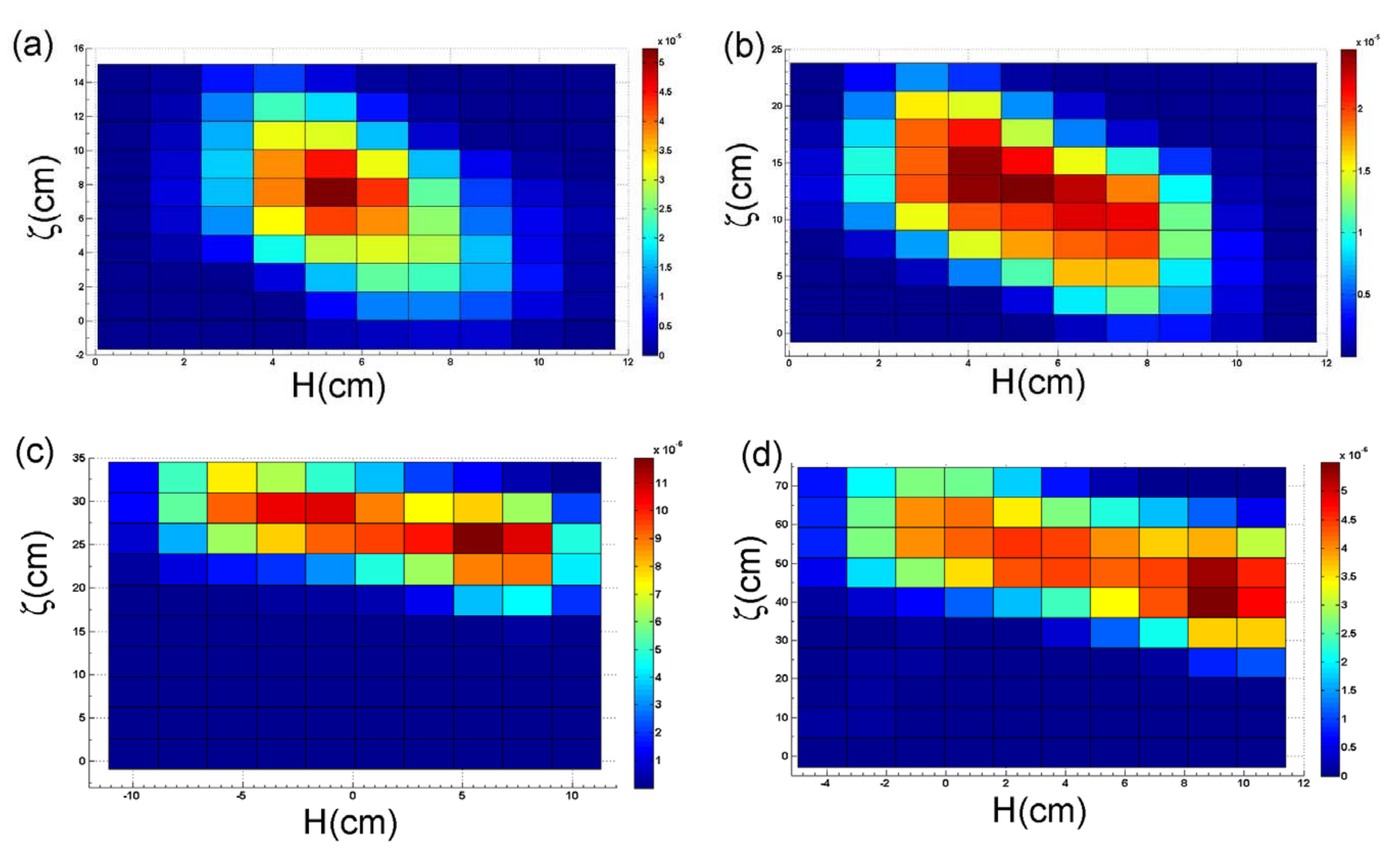

Experimental: solution blowing and co-blowing setups

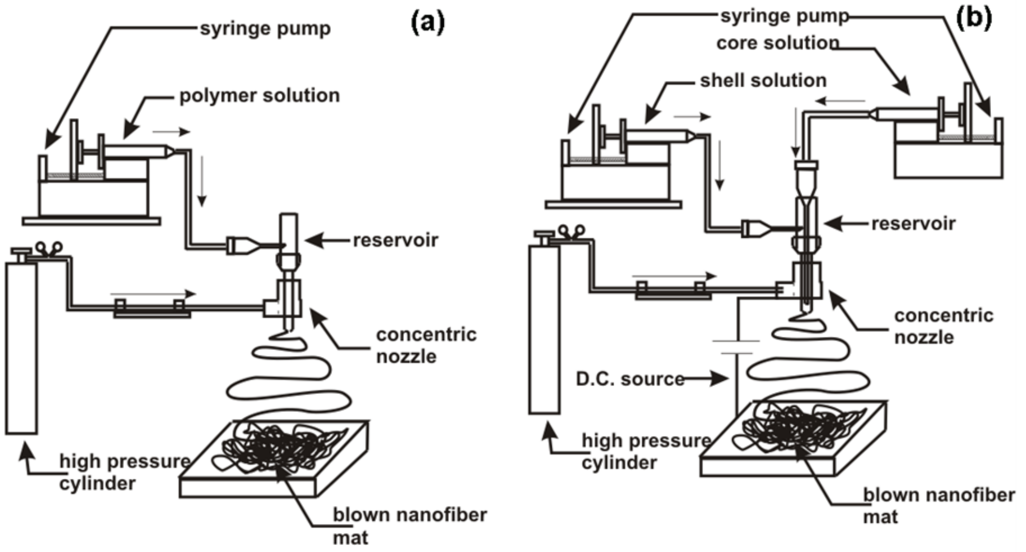

Mechanical & Industrial Engineering

Solution-blown polymer jet: Vigorous bending and flapping

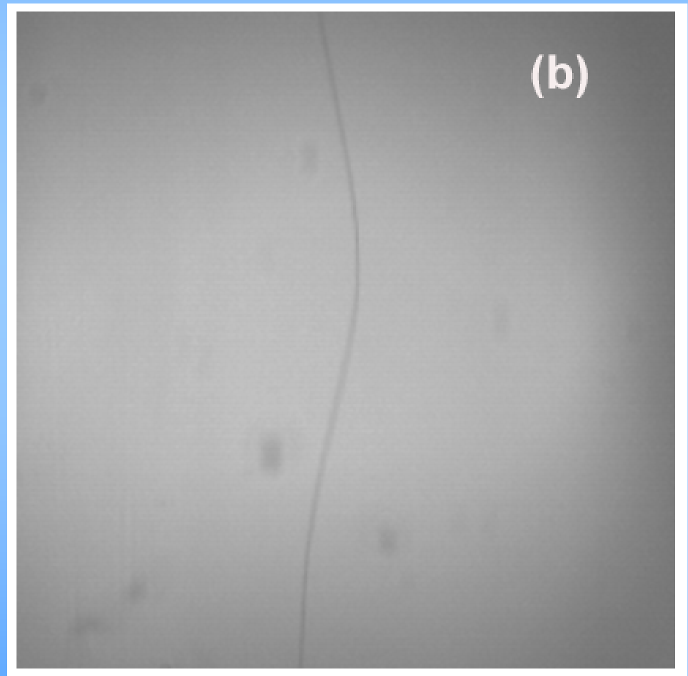

Mechanical & Industrial Engineering

Solution-blown and co-blown nanofibers and nanotubes

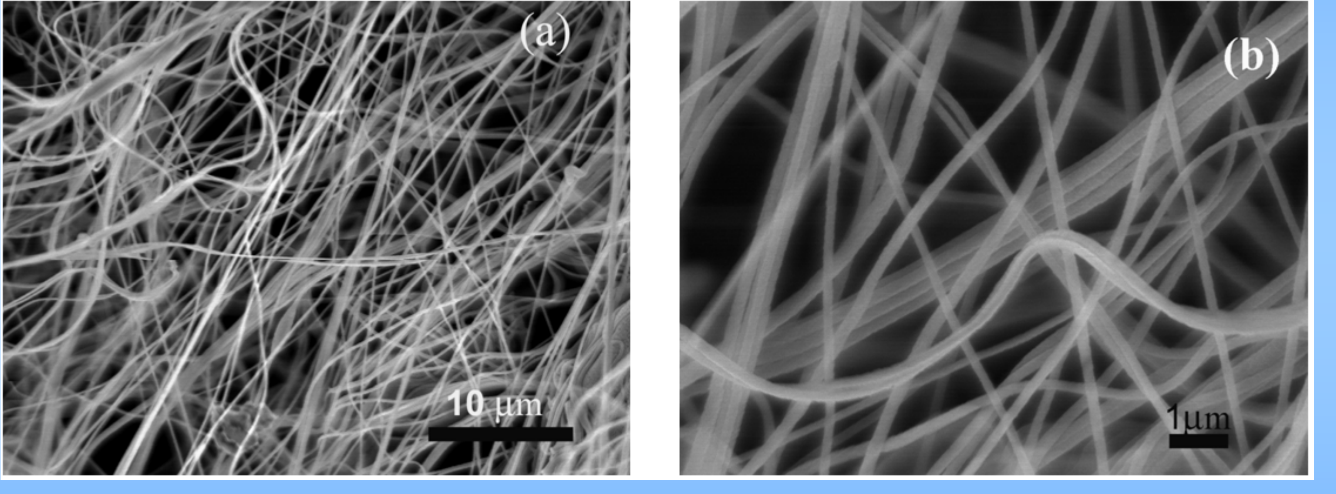

Monolithic PAN nanofibers

Mechanical & Industrial Engineering

Solution-blown and co-blown nanofibers and nanotubes

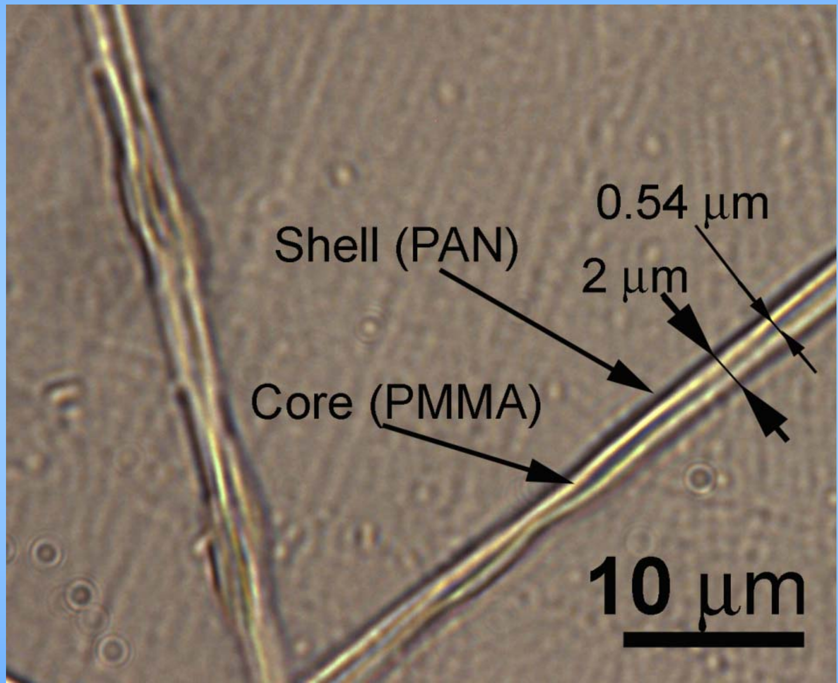

Optical image of PMMA-PAN core-shell co-blown fibers

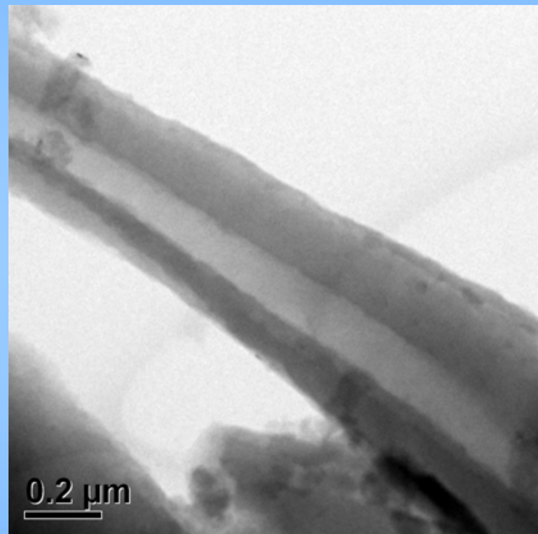

PMMA-PAN carbonized: Hollow carbon nanotubes

Mechanical & Industrial Engineering

Solution-blown monolithic nanofibers

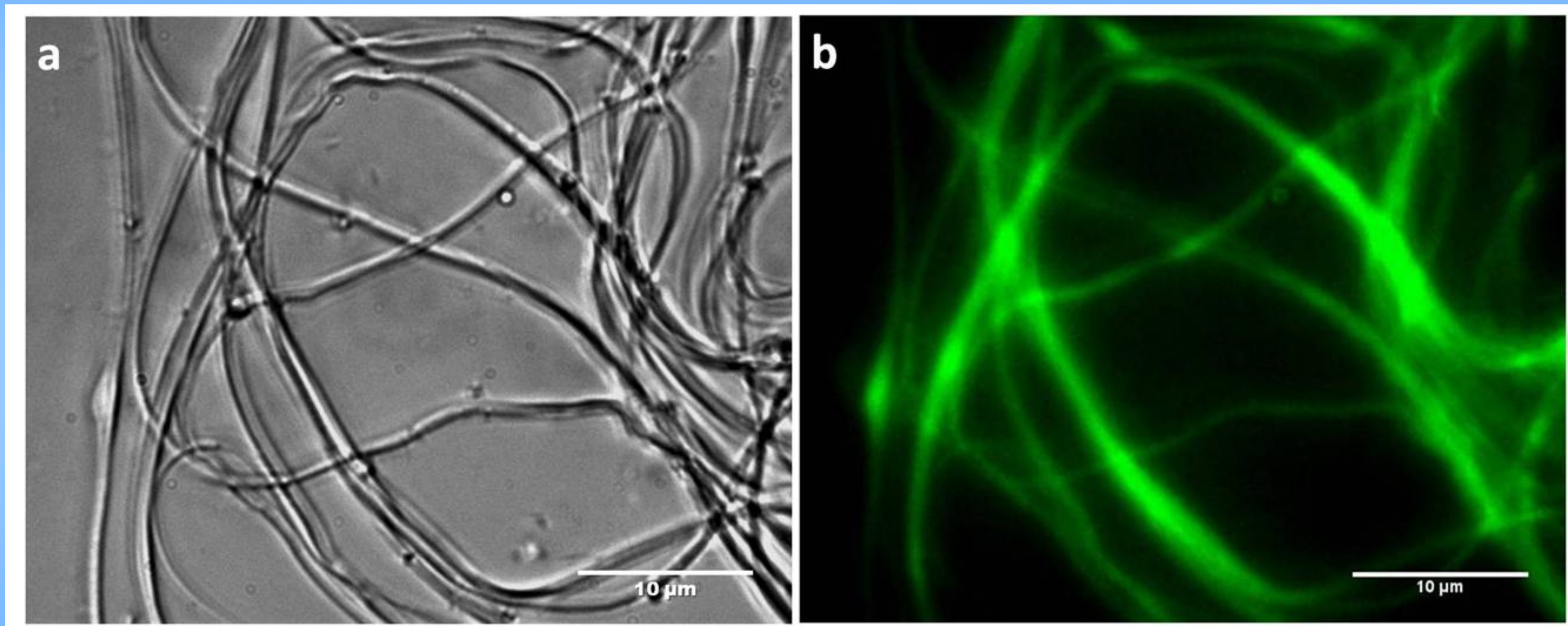

Solution-blown core-shell nanofibers

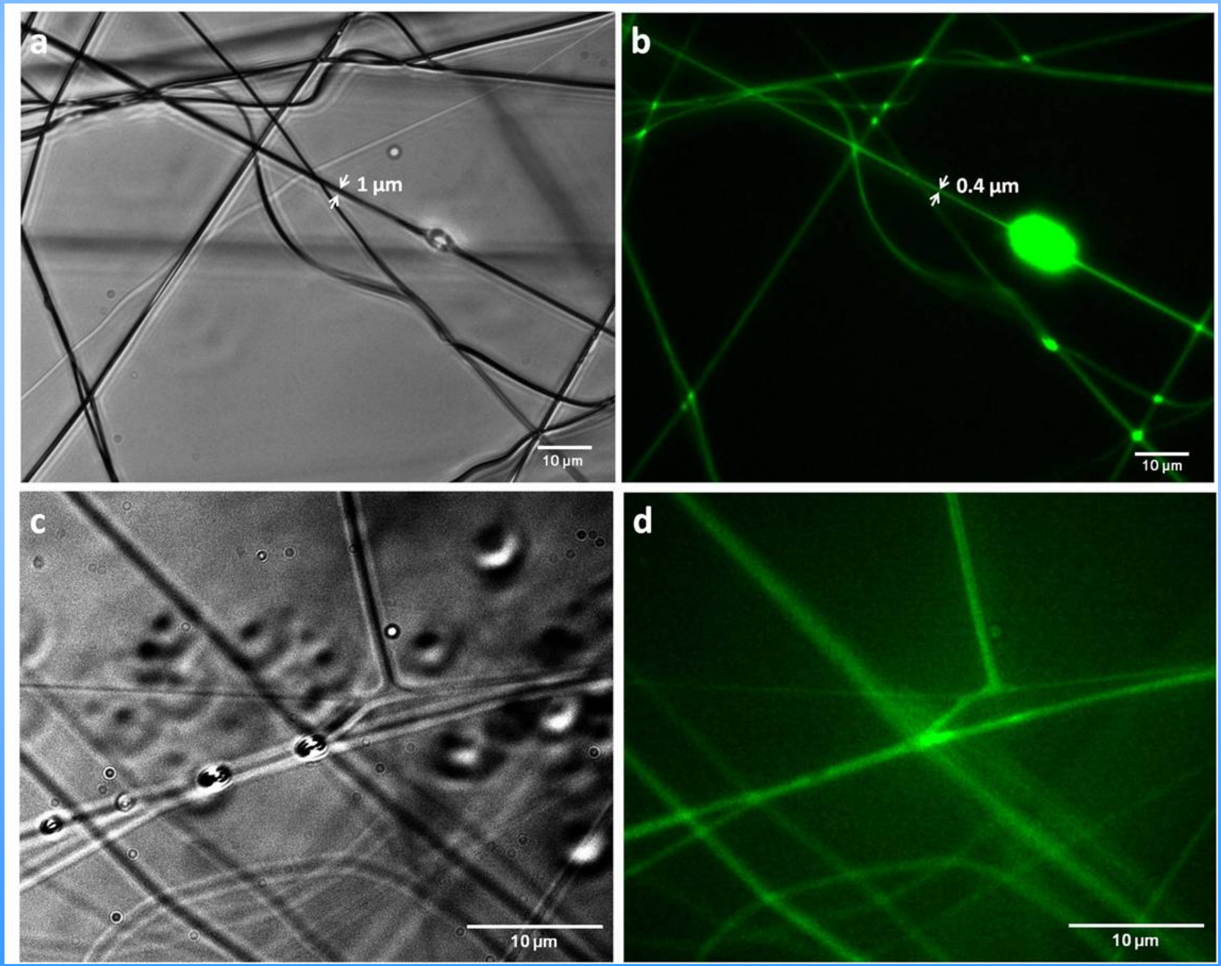

Mechanical & Industrial Engineering

Close Relatives

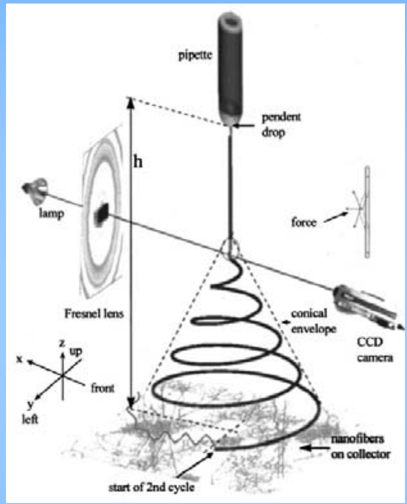

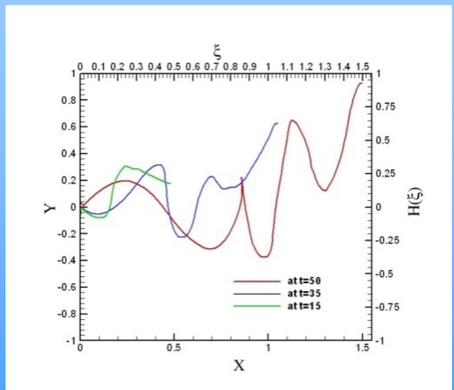

Sea snakes, electrospun and meltblown jets, and flame thrower napalm jets extract energy from the surrounding medium via bending